Thermo-hydraulic analysis of refinery heat exchangers undergoing fouling – Revision V1

E. Diaz-Bejarano[1], F. Coletti[2], and S. Macchietto[1,2]*

[1]Department of Chemical Engineering, Imperial College London, London SW7 2AZ, UK

[2]Hexxcell Ltd., Imperial College Incubator, Bessemer Building Level 2, Imperial College London, London SW7 2AZ, UK

Corresponding author: s.macchietto@imperial.ac.uk

Crude oil fouling severely affects energy efficiency and operations in refinery pre-heat trains. The use of historical plant data to estimate fouling and develop predictive models is the most practical approach to predict and assess the future state and performance of heat exchangers, cleaning schedules and other mitigation operations. A complete modelling framework is presented that brings together various dynamic models, some new formulations, and a method for the analysis and characterization of fouling and cleaning of heat exchangers based on thermal and hydraulic performance. The systematic approach presented allows: a) evaluating the fouling state of the units based on thermal measurements and pressure drops, if available; b) identifying the range of deposit conductivity that leads to realistic pressure drops, if those measurements are unavailable; c) estimating key fouling and ageing parameters; d) estimating the effectiveness of cleaning and surface conditions after a clean; e) predicting thermal performance with good accuracy for other periods/exchangers operating in similar conditions.

An industrial case study of exchangers at the hot end of a pre-heat train highlights the risks of fitting fouling models solely based on thermal effects and ignoring ageing, and the potential advantages of including pressure drop measurements. Performance is predicted in seamless simulations that include partial and total cleanings, covering an operating period of more than 1000 days.

Keywords: crude oil, fouling, thermo-hydraulic model, parameter estimation, cleaning, simulation, energy efficiency.

Introduction

The pre-heat train at the front end of refinery crude distillation units is severely affected by fouling, the undesired deposition of materials on the heat transfer surfaces[1]. The analysis of fouling, i.e. studying the time evolution and the factors influencing deposition, is a key activity to obtain insights into the underlying causes, predict the likely performance, evaluate the economic losses due to fouling, plan mitigation actions and cleaning, and design new heat exchangers and networks to operate under conditions that minimize fouling and increase energy efficiency[2–7].

The study of the dynamics of crude oil fouling has traditionally focused on (and is still dominated by) the development of correlations that capture the change in thermal fouling resistance, R_f, over time and as function of key design parameters and operating conditions. This value is usually calculated by using simplified, lumped models for heat exchangers (e.g. LMTD or ε-NTU method) and plant temperature and flowrate measurements[7]. The semi-empirical 'threshold' models, first proposed by Ebert and Panchal[8] to describe chemical reaction fouling, are by far the most widely used to quantify crude oil fouling in refineries, as discussed in several reviews over the past years[7,9–11]. Such fouling models fitted to lab data have had limited success in predicting fouling behaviour at the plant level. This has led to the direct use of plant data (temperatures and flowrates) to fit the adjustable parameters in fouling models. In industrial practice, this approach has become standard and is applied systematically without further consideration of oil type, deposit composition or fouling mechanism. In most cases, the results of the regression are not accompanied by a comprehensive statistical analysis. R_f and the standard calculation methods have been severely criticized (for instance, see discussions in refs.[7,12]). R_f-based models are subject to many simplifying assumptions and, as a result, have limited success in predicting long operation periods and are generally not portable to heat exchangers different from the one used in the fitting. Crittenden *et al.*[13] showed that typical measurement errors may lead to errors in the order of 20% in R_f when using standard calculation methods. Smoothing techniques [14], sophisticated filtering

methods [15] and improved methods for calculation of R_f [6] have been proposed to reduce the scattering of calculated R_f time-series and facilitate the analysis.

In literature, the estimation of fouling parameters is typically carried out using calculated R_f and some type of regression analysis (see as examples refs.[16–20]). A recent example, presented by Costa *et al.*[20], involves the application of various types of optimization algorithms (Simplex, BFGS, Genetic Algorithm). The goodness of the fitting was evaluated by the average relative error.

An alternative approach uses Artificial Neural Networks (ANN) algorithms to produce empirical fouling models[21–23]. This approach allows finding correlations between multiple inputs (e.g. operating conditions, composition, etc.) and the desired model outputs (usually fouling resistance). However, such empirical models are specific to the particular configuration of the heat exchanger, the range of operating conditions and oil type, and require re-estimation if any of those changes significantly.

In the approaches above, crude oil fouling is treated as a lumped resistance, neglecting spatial, compositional and flow-renstriction effects. These features are essential to adequately capture both thermal and hydraulic impact of fouling on heat exchanger performance[24]. The hydraulic effect is ignored in most fouling analysis work, but it is often the limiting one due to which heat exchangers are dismantled for cleaning[25].

From the modelling point of view, considering these aspects implies moving beyond the simplistic R_f description of fouling towards more rigorous approaches that account for flow restriction, local effects and distinguish between modelling of the deposition phenomena and the deposit itself. Advances in the modelling of crude oil fouling deposits and their thermal and hydraulic impact are reviewed in ref.[24]. Along those lines, Coletti and Macchietto[26] proposed the use of measured inlet temperatures and flowrates as inputs to a *dynamic*, *distributed* thermo-hydraulic heat exchanger model with a *distributed* deposition rate (adapted threshold model), and used the measured outlet temperatures to estimate the fouling parameters. They used a parameter estimation method based on the Maximum Likelihood formulation for *dynamic* systems[27]. This approach has several advantages. First, primary measurements are used to fit the parameters, avoiding the uncertainty, simplifying assumptions and error propagation

introduced in the calculation of lumped fouling resistances. Second, standard statistical analyses are used to evaluate the quality of the estimation. Finally, the formulation allowed the inclusion, for the first time, of *local* deposit ageing (reflecting the distinct temperature-time history at each point in the deposit) in the analysis of crude oil fouling rates, with ageing was assumed to follow Arrhenius-type kinetics.

In order to decouple fouling rate from the evolution of the composition of the deposit, additional measurements to flow rates and temperatures are required. Direct analysis of the composition is only possible if samples are collected during the dismantling of the units for cleaning, which only happens every few months or even years. In this context, pressure drop measurements are a promising alternative to, first, directly measure the hydraulic impact of fouling, and second, indirectly measure the amount of material depositing. In order to introduce such measurements in the analysis, suitable models that consider the thermal and hydraulic impact of fouling are necessary.

The use of pressure drop measurements to fit crude oil fouling models from plant data has not been reported in the literature. This is imputed to the lack (or inaccessibility) of such measurements for individual exchangers in refineries. While this is often the case, some refineries do have and collect pressure drop measurements .

Thermo-hydraulic models, either lumped[16] or distributed[26], have been used to predict the impact of fouling on pressure drop based on fouling models previously fitted using thermal measurements (either primary temperature measurements or calculated fouling resistances). However, these hydraulic models have not been validated with respect to pressure drop predictions or used to assist in parameter estimation. Nonetheless, the importance of pressure drop measurements for individual heat exchangers has been highlighted in multiple theoretical studies as a way to help infer the impact of the deposit's thermal-conductivity, to establish partial cleaning efficiency, as a key factor to assess flow (mal) distribution in networks and support throughput maintenance decisions, and as important factor to take in consideration in heat exchanger design and network synthesis[16,24,28–32].

One of the main applications of predictive fouling models is cleaning scheduling, for which extensive literature has been published over the past years (see, for instance, the review by Diaby *et al.*[33]). Models used in cleaning scheduling normally treat the fouling deposit as a thermal resistance R_f, describe the fouling rate with linear, asymptotic or (at best) threshold models, and describe heat exchangers as lumped systems. Such works are subject to the fundamental lack of predictive ability associated to the simplified fouling, cleaning and heat exchanger models used in the problem formulation. Consequently, even if an 'optimal' cleaning schedule is found, its application to actual facilities does not necessarily guarantee an optimal (or even improved) solution. Cleaning is commonly assumed to completely restore the original performance (total cleaning) and cleaning times are fixed. However, the effectiveness of a cleaning depends on cleaning method (usually mechanical or chemical) and the properties of the fouling layer produced thus far. An early attempt to include cleaning effectiveness in the analysis of fouling was reported by Radhakrishnan *et al.*[21]. They introduced the 'peak efficiency', defined as the maximum *cleanliness factor* after chemical cleaning, as a training variable in their empirical ANN-based model. The peak efficiency was obtained from plant data and was not related to the composition or coking state of the deposit. In a later work, Ishiyama *et al.*[34] used their simple double-layer deposit model to explicitly introduce the lumped deposit ageing model of Ishiyama *et al.*[35] in the cleaning scheduling optimization problem. This approach, to our knowledge, has not been validated against experimental or plant data and the ageing rates are based on parametric, theoretical studies. A more rigorous estimation of the efficiency of a chemical cleaning could be accomplished by defining a cleaning rate as a function of cleaning operating conditions (e.g. temperature, velocity), type and concentration of chemical ageing, and state of the deposit (coking, composition). Modelling efforts along these lines have been reported in the food industry and, particularly, in milk fouling[36].

In a recent work, Diaz-Bejarano *et al.*[24] presented a new dynamic model for the description of crude oil fouling deposits that overcomes many of the above limitations. It has the ability to capture the detailed time-conditions history at each point in the deposit layer by including multicomponent species, multiple reactions and deposition/removal fluxes at a moving oil/deposit boundary. This formulation allows simulating cleaning as a dynamic process, linking cleaning effectiveness to the deposit condition,

and dynamically simulating fouling-cleaning sequences considering time as a continuous, rather than discretized variable. The model was implemented within a single heat exchanger tube, permitting the simultaneous evaluation of the impact of fouling on both heat exchange and pressure drop.

In this paper, the deposit model by Diaz-Bejarano *et al.*[24] is implemented within the dynamic, distributed heat exchanger model by Coletti and Macchietto[26]. A methodology is proposed to extract information about the fouling status of the heat exchanger, fit fouling models for prediction based on historical plant data, and estimate the effectiveness of partial cleanings. The modelling framework and method are applied to a case study comprising two industrial heat exchangers at the hot end of a refinery, where chemical reaction fouling and an organic deposit undergoing ageing are likely to provide a good representation of the system.

Modelling framework

The modelling framework is based on the description of the shell-and-tube heat exchanger as a dynamic and distributed system developed by Coletti and Macchietto[26] and currently implemented in Hexxcell *Studio*™ [37]. This model includes a thermal-hydraulic description of heat exchange between tube and shell fluids and pressure drop on both sides (including the hydraulic effects of headers and nozzles[38,39]), and the physical properties of the fluids as function of fluid characteristics and local temperature. Using this framework, various implementations of the fouling layer are considered, each with different level of detail in the description of the deposit, purpose, and applications. This hierarchical modelling framework is schematically shown in Figure 1 for four increasingly simplified approximations of the deposit model (‘modes’). The main equations for these modes and boundary conditions between the deposit, tube-side flow and wall sub-models are summarized in Table 1. Here, fouling is assumed to be limited to inside the tubes (which is appropriate for the example considered later, where shell-side fouling is negligible). Further details on the development of the heat exchanger model and detailed deposit model can be found in ref.[26] and ref.[24], respectively.

Fouling deposit model: simplified modes

The model can be used in four different modes which correspond to the different levels of simplification of the deposit model. These are, in decreasing degree of complexity:

Mode I: **Distributed, multi-component:** full model as in ref.[24] accounting for local growth or decrease of the deposit thickness (δ_l) depending on deposition and removal fluxes at a moving boundary between deposit layer and flowing crude oil. The composition determines the physical properties of the layer, such as thermal-conductivity (λ_l). In this mode, the model is used to *predict* the performance of the heat exchanger as the deposit builds-up over time, from given (time-varying) inlet conditions (hot and cold streams temperature and flowrate) and crude oil properties. The net deposition rates ($n_{f,i}$) determine the spatial distribution of the fouling layer inside the heat exchanger. If a cleaning action is undertaken, the cleaning rate ($n_{Cl,k}$) determines the amount of deposit removed. If the cleaning is partial, the remaining layer is considered to be unaffected by the cleaning activity and, therefore, its concentration profile conserves the previous history. The local rate of change in thickness in a pass *n* of the heat exchanger ($\dot{\delta}_{l,n}$) is defined as:

$$\dot{\delta}_{l,n}(z) = (1 - b_{clean}) \sum_{i}^{NC} \frac{1}{\rho_i} n_{f,i,n}(z) - \sum_{k=1}^{NCl} b_k \frac{1}{\rho_{l,n}(z,1)} n_{Cl,k,n}(z) \qquad (1)$$

where b_{clean} is a 0-1 variable defining if any cleaning is taking place and b_k is a binary variable which indicates if cleaning method *k* is active (b_k=1) or not (b_k=0).

Mode II – **Uniform thickness and thermal conductivity:** a simplification of the model used in Mode I featuring spatially uniform deposit thickness and conductivity throughout the unit. This mode can be used: a) to infer an *apparent* thickness and conductivity from measured inlet and outlet plant data; b) to predict duty and pressure drop from given inlet conditions, deposit thickness and conductivity.

Mode III - **Apparent fouling resistance**: the deposit is modelled as a uniform resistance to heat transfer. This description ignores the gradual restriction of the flow area as fouling builds up and its impact on the tube-side heat transfer coefficient (hence the apparent) and pressure drop (calculated as

in clean conditions). The fouling resistance is referred to the inner tube surface area. It is noted that this fouling resistance is calculated with the distributed heat exchanger model, avoiding simplifying assumptions in physical properties, heat transfer coefficients or temperature distribution in traditional approaches (e.g. LMTD models)[7].

Mode IV – **Clean**: a further simplification of the model used in Mode I that neglects deposition altogether. It is used to predict the performance of the heat exchanger in clean conditions over time for given (time-varying) inlet conditions.

Solution types

In previous works[24,26], the heat transfer system (either a tube or a heat exchanger) required inlet conditions of temperature and flowrate for each stream as inputs and calculated, as the deposit developed, the outlet temperature (thus, heat duty) and pressure drop for both tube and shell-side fluids. These inputs and outputs were defined to use the deposit models as a predictive tool. However, the choice of degrees of freedom may be different with the simplified deposit versions and variables that were originally defined as model outputs are used as inputs and *vice versa*. Four solution types can be considered depending on the choice of degrees of freedom (summary in Table 2):

i) Prediction (P): calculation of duty and pressure drop as function of inlet conditions and deposit characteristics (either fixed or dynamic). Applicable to all modes (I, II, III, IV).

ii) *Q*-Prediction (QP): calculation of deposit thickness and heat duty as function of measured pressure drop and thermal-conductivity. This solution type can be used to check the potential thermal impact of different types of deposits based on pressure drop measurements.

iii) Δ*P*-Prediction (PP): calculation of deposit thickness and pressure drop as function of measured duty and thermal conductivity. This solution type can be used to check the potential impact of different types of deposits based on heat duty measurements.

iv) Analysis (A): calculation of fouling deposit characteristics as function of measured inlet and outlet conditions (‘inverse problem’). Applicable to modes II and III:

a. Mode III: fix heat duty to calculate R_f. This solution type requires, at least, flowrates, inlet and outlet temperatures for one side and inlet temperature for the other.
b. Mode II: pressure drop measurements are used to calculate the thickness, then heat duty is used estimate the corresponding conductivity. This solution type requires both thermal and hydraulic information.

In Prediction type calculations, pressure drop and heat duty are calculated as function of the inlet conditions of temperature and flowrate (for shell and tube sides) and fouling deposit characteristics (which determine the resistance to flow and heat transfer). In Analysis type calculations, duty and pressure drop come from measurements. Pressure drop may be an actual measured variable. The 'measured' heat duty refers to the sensible heat duty calculated from measured flowrate and inlet and outlet temperatures. For instance, the tube-side heat duty, Q_t, is given by:

$$Q_t = \dot{m}_t \int_{T_{in,t}}^{T_{out,t}} C_{p,t}(T) dT \tag{2}$$

where $\dot{m}$ is the mass flowrate, T is the fluid temperature, C_p is the specific heat capacity, and subscripts *t*, *in* and *out* refer to tube-side fluid, inlet and outlet, respectively.

In theory, the heat balance should close and the heat duty of the shell and tube-side fluids should be equal. In practice, however, there may be some disagreement due to a combination of measurement error and inaccurate estimation of the physical properties.

In the following, the nomenclature of the layer mode and solution type used at each stage of the analysis is indicated by the layer mode following by the acronym of the solution type (in brackets in the definitions above). For instance, Mode III solved in analysis type is referred to as Mode III-A, Mode II solved in ΔP-prediction is Mode II-PP, etc. Modes I and IV can only be used with prediction type, and therefore are just referred to with the mode number.

Predicted, average and apparent values

For the full deposit model (Mode I) the deposit thickness and conductivity evolve over time as function of local conditions, fluxes of fouling species and transformations such as ageing or removal

by shear or cleaning. Only if the functionality of the various fluxes and transformations are known, it is possible to calculate these *predicted* spatially distributed conductivity and thickness.

The measurements usually available correspond to entry and exit operating conditions: flowrate, inlet/outlet temperatures and (less frequently) tube-side pressure drop. Based on those measurements in isolation (without deposition models), it is not possible to calculate the distributed characteristics of the deposit. A uniform layer such as that in Mode II is more appropriate. The deposit thickness and conductivity obtained with this deposit model (and A, QP or PP calculation types) are therefore *apparent* properties of the layer, since they correspond to the properties that can be inferred merely providing entry/exit information and geometry to the distributed heat exchanger model. These apparent values capture the overall contribution of the spatially distributed deposit thickness and conductivity to pressure drop and heat exchange. The apparent quantities also include model errors if the assumptions in the hydraulic model are not correct. For instance, the apparent thickness will include all the effects influencing pressure drop (such as changes in roughness, uneven tube blockage, etc.)[16,40–42], and not only the flow restriction effect accounted for in the model[26].

If the behaviour of the system is well described by the model and its assumptions, the *predicted* variables should provide a good representation of the actual system. In an ideal situation, it should be possible to find equivalence between the *predicted* and *apparent* values. The following expressions are proposed for the *average* deposit properties, calculated from the distributed *predicted* deposit layer:

- The *average thickness* is calculated as the distributed thickness integrated over the tube length, and averaged for the number of passes (N_p) and shells (N_s):

$$\delta_{ave} = \frac{1}{N_s}\sum_{s=1}^{N_s}\left[\frac{1}{N_p}\sum_{n=1}^{N_p}\left(\frac{1}{L}\int_0^L \delta_{l,n}(z)dz\right)\right]_s \tag{3}$$

- The *average effective conductivity* is calculated as the distributed effective conductivity integrated over the tube length, and averaged for N_p and N_s:

$$\lambda_{eff,ave} = \frac{1}{N_s}\sum_{s=1}^{N_s}\left[\frac{1}{N_p}\sum_{n=1}^{N_p}\left(\frac{1}{L}\int_0^L \lambda_{eff,n}(z)dz\right)\right]_s \tag{4}$$

An *effective* conductivity at a location *z* in the axial direction is defined as the lumped value that results, for a given deposit thickness, in the same heat transfer resistance as the actual radially distributed layer:

$$\lambda_{eff,n}(z) = \frac{q''_{w,n}\big|_{r=R_i}(z) R_i \, ln\left(\frac{R_i}{R_{flow}(z)}\right)}{\left(T_{l,n}\big|_{r=R_{flow}}(z) - T_{l,n}\big|_{r=R_i}(z)\right)} \tag{5}$$

where $q"_{w,n}$ is the heat flux at the tube wall, T_l is the local temperature in the deposit layer, R_i is the inner tube diameter, and R_{flow} is the flow radius.

Note that the average effective conductivity is different from the arithmetic average conductivity:

$$\lambda_{ave} = \frac{1}{N_s}\sum_{s=1}^{N_s}\left[\frac{1}{N_p}\sum_{n=1}^{N_p}\left(\frac{1}{(R_i - R_{flow})L}\int_0^L \int_{R_{flow,n}}^{R_i} \lambda_{l,n}(z,r)dr\,dz\right)\right]_s \tag{6}$$

Finally, the apparent fouling resistance calculated with Mode III-A does not take into account the impact of flow constriction on the tube-side heat transfer coefficient. In order to compare that apparent coefficient and the fouling resistance imposed by a distributed fouling layer, the following calculation is required (referred to as *average* resistance, for coherence with previous definitions):

$$R_{f,ave} = \frac{1}{N_s}\sum_{s=1}^{N_s}\left[\frac{1}{N_p}\sum_{n=1}^{N_p}\left[\frac{1}{L}\int_0^L\left(R_{f,l,n}(z) + \frac{1}{h_n(z)}\right)dz\right] - \frac{1}{N_p}\sum_{n=1}^{N_p}\left(\frac{1}{L}\int_0^L \frac{1}{h_{n,c}(z)}\,dz\right)\right]_s \tag{7}$$

where h_n and $h_{n,c}$ are the tube-side heat transfer coefficient in fouled and clean conditions, respectively. $h_{n,c}$ is determined by solving the heat exchange model with layer Mode IV and the same inlet conditions. The local fouling resistance, $R_{f,l,n}(z)$, and $h_n(z)$ are obtained in the full simulation with Mode I. The local fouling resistance referred to the inner tube surface area is:

$$R_{f,l,n}(z) = \frac{T_{l,n}\big|_{r=R_{flow,n}}(z) - T_{l,n}\big|_{r=R\_i}(z)}{q''_{w,n}\big|_{r=R_i}(z)} \tag{8}$$

Thermo-hydraulic analysis method

The methodology used for the study of crude oil fouling involves the following six steps:

1) System definition

The first step is to set up the model including: a) heat exchanger geometry and flow configuration; b) physical properties of the fluids.

The physical properties may be calculated using thermodynamic packages or correlations. In this work, established correlations[43] are used to calculate density, heat capacity, viscosity and conductivity of the crude oil and heating fluid as function of local temperature. The advantage of such correlations is that they rely on a small number of characteristic parameters (API gravity, mean average boiling point, and kinematic viscosity at 38ºC) for each oil type.

2) Data filtering and error analysis

Data points with gross errors must be eliminated from plant data since these may compromise the robustness of the simulation and affect the value of the estimated parameters. Data reconciliation may be necessary if part of the data is missing or if the heat balance presents large errors.

3) Dynamic analysis of fouling state

First, the base-line for clean conditions is compared with the plant data. This can be done either comparing plant data with the predictions of Mode IV, with Mode III-A or Mode II-A (if ΔP is available). A significant deviation from clean conditions at the initial stages of an operating period could be due to: i) inaccuracy of the correlations used for prediction of physical properties, correlations for heat transfer coefficients and friction factor, and other assumptions in the model; ii) heat exchanger initially not clean; iii) non-reported operations such as bypasses or others. Significant deviations from the baseline should be corrected since they will affect the analysis and the estimation of fouling parameters. The correction method will depend on the specific case in hand. Actual records of the dates and types of cleaning and visual inspection of the exchanger state before and after the cleaning are valuable information that can help at this stage.

Once the initial conditions for the period under study have been settled, the analysis of the fouling state of the heat exchanger can be carried out by using the Analysis solution and the simplified modes described in the previous section. Two main scenarios may be considered:

a) If *pressure drops are not available* (the most common case), Mode III-A is used to calculate the apparent fouling resistance over time. The information provided can be used to identify operating periods and cleanings based on the plant data.

b) If *pressure drops are available*, Mode II-A is used to provide the apparent thickness and conductivity over time. This can also be used to identify cleanings (complementary with R_f), but gives more insights into the likely nature and evolution of the deposit.

If scenario (a) applies, there is still the possibility of using Mode II-PP, i.e. given the thermal performance (heat duty), to evaluate the hydraulic performance (pressure drop) for fixed values of average deposit conductivity. This use of the model as a pressure drop 'soft sensor' may provide insights into the possible range of conductivities in the heat exchanger that lead to 'reasonable' pressure drops. Given the general lack of pressure drop data, it is difficult to establish what reasonable pressure drops to expect. As a general rule of thumb, a maximum ratio $\Delta P/\Delta P_c \approx 5$ is taken as reference value, as indicated in ref.[16].

4) Selection of deposition rate model

With the information obtained from the previous analysis, the next step is either to: i) develop a deposition model as a function of the operating conditions, crude oil composition and deposit composition, for which extensive amount of data is required; or, alternatively, ii) to select available correlations if the type of deposit has been identified or can be guessed with some confidence. The functionality in the fouling rate equation (or equations, if various foulants have been identified and de-correlated) will eventually determine the distribution of the fouling deposit along the tubes, passes, and shells of the heat exchanger.

5) Estimation and testing of fouling parameters

Once a suitable fouling rate equation has been identified, the estimation of the fouling parameters is carried out with Mode I by fixing the model inputs (measured inlet temperatures and flowrates) and fitting the model to measured outputs.

Generally, only thermal information is readily available, and therefore the estimation is performed by fitting the outlet temperatures (as in ref.[26]). If pressure drops were available, these could be used as additional measurements. In this work, the gPROMS parameter estimation facility[27], based on the Maximum Likelihood approach, is used to obtain the optimal estimates of the parameters.

Once estimated, the ability of the fouling models to describe the system should be tested against other data sets.

6) Analysis of partial cleanings

The analysis of partial cleaning requires the fouling rates and the evolution of the deposit to be well defined. As a first approach, the cleaning rate models by Diaz-Bejarano *et al*.[24] can be used to link the amount of deposit removed and the composition of the remaining layer. Correct identification of the cleaning effectiveness enables accurate predictions of plant data after partial cleaning, if the fouling and deposit parameters are correct and no other unrecorded process operations (e.g. bypasses, changes in feedstock, etc.) take place.

Case study

The case study involves two heat exchangers at the hot end of a refinery preheat train (E02AB and E05AB, Figure 2), located downstream of the desalter and flash drum. These heat exchangers have two shells each, operate under similar conditions, with the same fluids (crude oil and atmospheric residuum). Visual inspection during dismantling for cleaning showed substantial fouling on the tube-side, whilst it was reported to be negligible on the shell-side. Therefore they are considered suitable candidates for the application of the heat exchanger model.

The objective of the case study is to investigate the fouling behaviour in units E02 and E05:

a) Analyse fouling state over time.
b) Extract fouling and ageing parameters using the information for one of the periods (defined as the time elapsed from a cleaning to the next cleaning) starting from clean conditions.
c) Test the prediction capabilities on the other periods starting from clean conditions.

d) Extract information on partial cleanings and simulate, seamlessly and under time-varying inputs, the thermal-hydraulic performance through the cleanings.

System definition

Heat exchangers E02 and E05 have the same geometry. The main parameters are reported in Table 3. The physical properties of the oil and heating fluid were determined by combining information from the refinery and open literature databases, as detailed in ref.[44]. The characteristic parameters are summarized in Table 3.

Data filtering and error analysis

The data set covers about three years of operation for which average daily data is available. For each exchanger, data include inlet and outlet temperatures and flowrates for both fluids (Figure 3). Pressure drop information was not available.

Data points with gross errors were filtered out, as detailed in ref.[44]. After filtering, there is a residual error in the heat balance that is associated to errors in the measurements and potential mismatch between the correlations and the actual physical properties (calculation of heat capacity and density). In order to provide a single value of 'measured' heat duty over time, the average between the heat duty calculated only with shell-side measurements and the heat duty calculated only with tube-side measurements was taken for the analysis that follows. Assuming that the inputs to the model are correct (T_{in}, $\dot{m}$), the errors in the heat balance are translated into an error on the outlet temperatures of ±1.5%. This error is taken as the reference to establish the goodness (or quality) of the fit of the model.

Dynamic analysis of fouling state

Based on raw plant measurements (Figure 3), it is difficult to evaluate the fouling state and identify the time when cleanings were performed. Instead, Mode III-A was used to calculate the apparent fouling resistance and evaluate the fouling state of the heat exchangers with respect to the clean baseline. The

results are shown in Figure 4(a). Three periods (P1, P2, P3) can be clearly identified for each unit leading to the schedule in Table 4. The heat duty in each heat exchanger is also reported (Figure 4b).

Total cleanings (TC) were established based on: i) the extent of the drop in fouling resistance to approximately clean conditions; and ii) the time in plant data taken to re-start fouling build-up (1 to 3 weeks). This analysis is in agreement with the information reported by the refinery for mechanical cleanings. According to visual inspection, fouling was observed to occur on the tube-side and mechanical cleaning led to complete removal of the deposits.

Partial cleanings (PC) are detected as sudden and significant drops in fouling resistance that differ from the usual oscillation in the apparent fouling resistance during operation. The duration of the cleaning time (2 to 4 days) indicates a chemical cleaning method. The final cleaning in E02 (PC2) was confirmed to be a chemical cleaning, but no records were provided for the other two PC in Table 4. Given the similarity between these partial cleanings, it was assumed that all of them correspond to chemical cleanings.

The first complete period starting from clean conditions (E05-P1) was selected as estimation period for fitting of the fouling parameters. The other two periods starting from clean conditions (E05-P3, E02-P2) are then used to test the predictive capabilities of the model. Finally, the effectiveness of the partial cleanings PC1 for each heat exchanger as function of deposit composition and extrapolation beyond such cleaning actions are investigated.

Selection of deposition rate model

Given the location and observations reported, an organic fouling is assumed to be the main cause of fouling (as defined and modelled in ref.[24]). Fouling of organic matter at high temperature is well known to increase with temperature and decrease with flow velocity. As a result, a functionality of the type suggested by Panchal *et al.*[45] was assumed for the net deposition rate. The fresh deposit was assumed to be of a gel form with thermal conductivity of 0.2 $Wm^{-1}K^{-1}$ and to undergo ageing at high temperature. The deposit is totally converted to coke when it reaches a final conductivity of 1 $Wm^{-1}K^{-1}$. These are the typical reference minimum and maximum values of conductivity assumed for organic

gel and coke in preheat train heat exchangers (see refs.[35,46,47] for details). Therefore, two components (gel and coke) and a chemical reaction (ageing) are defined for the mass balance in Mode I. As a result, the three main phenomena affecting the dynamic behaviour of the fouling layer are: deposition, deposition-offsetting (removal or suppression, as discussed by Diaz-Bejarano *et al.*[48]) and ageing. The same two components and chemical reaction are defined for the mass balance in Model III. The net deposition and ageing rates are assumed to be well described by the following functional forms[24]:

$$n_{gel,n}(z) = \alpha' Re_n(z)^{-0.66} \mathrm{Pr}_n\,(z)^{-0.33}\, exp\left(\frac{-E_f}{RT_{film,n}(z)}\right) - \gamma' \tau_{w,n}(z) \tag{9}$$

$$n_{\,coke}(z) = 0 \tag{10}$$

$$r_{a,n}(z, \tilde{r}_l) = A_a \exp\left(-\frac{E_a}{R_g T_{l,n}(z, \tilde{r}_l)}\right) c_{l,gel,n}(t, \tilde{r}_l) \tag{11}$$

The net deposition of organic gel is given by the difference betweeen the deposition term (positive term in Eq. (9)) and the deposition-offsetting term (negative term in Eq. (9)). Organic coke is assumed to be formed in-situ as a result of ageing of the gel fraction.

As a preliminary step to the estimation of the fouling parameters with Mode I, Mode II-PP was used to calculate the ΔP under a number of constant conductivity scenarios in order to establish the range of conductivity that lead to realistic hydraulic performance. This was carried out by using the heat duty in Figure 4 as input and fixing a value of thermal-conductivity. The deposit thickness, which is an output of this Mode, and the input thermal conductivity correspond to apparent quantities. The predicted ΔP, normalized with respect to pressure drop in clean conditions (ΔP_c, obtained by running Mode IV), is shown in Figure 5 for E05AB-P1 for various thermal-conductivities within the range established for organic deposits. A deposit with negligible ageing (0.2 $Wm^{-1}K^{-1}$) leads to moderate impact on the hydraulic performance, with a maximum ratio $\Delta P/\Delta P_c \approx 2$. A fully coked deposit (1 $Wm^{-1}K^{-1}$) leads to a dramatic impact on the hydraulic performance which seems unrealistic, with $\Delta P/\Delta P_c \approx 5$ reached 76 days after total cleaning. A range of conductivities that lead to reasonable pressure drops can be established between 0.2 – 0.4 $Wm^{-1}K^{-1}$, for which the maximum $\Delta P/\Delta P_c$ remains < 5 throughout P1. Based on the previous results, the hypothesis of organic mechanism as main cause of fouling seems to be confirmed. It also indicates that the effect of ageing on the deposit thermal-conductivity, if it happens at all, is moderate.

If ageing occurs, there will be a conductivity profile varying radially, axially and for each pass and for each shell, and evolving over time[24,26]. It is difficult to determine, a priori, the actual extent and rate of ageing in the deposit. Consequently, the ageing parameters were selected as part of the unknown set of parameters that need to be fixed or estimated in the next section.

Estimation of fouling parameters and evaluation of ageing rates

Parameter estimation results

The following parameters in the net deposition and ageing models are unknown: fouling parameters α', E_f, and γ'; and ageing parameters A_a and E_a. The estimation of the unknown parameters was performed using data for the entire E05AB-P1 (349 days), by fixing the inlet conditions and fitting the model to the *outlet temperatures*. A relative variance model with a value of 0.015 (i.e. 1.5%) was used for tube and shell temperatures, based on the previous error analysis. The final estimation strategy was decided based on preliminary sensitivity, correlation and parameter estimation analysis[44]:

- A_a and γ' lead to similar response in the outlet temperatures and cannot be independently estimated (high correlation).
- α' and E_f are highly correlated. Rearrangement of the Arrhenius equation (as recommended in ref.[49]) did not reduce the correlation.

The final strategy consisted on estimating parameters α' and γ' for various pre-fixed values of A_a in the interval 0 – 0.01 s^{-1} (Sets A-E)[47]. E_a was fixed to 50 kJ mol^{-1} based on ageing parametric studies[47] and E_f to 28.5 kJ mol^{-1} based on reported values for the correlation by Panchal *et al.*[45] in refs.[16,26].

The results of the parameter estimation are reported in Table 5. In all cases a good fit was achieved (χ^2 test passed). The lack-of-fit test shows an increasingly better fit for greater values of A_a. The t-test indicated good confidence in the value of α' and was also passed at the 95% confidence level for γ' but with wider confidence intervals (except for Set D). High correlation was reported between α' and γ', increasing marginally with decreasing A_a. As observed in Table 5, the value of γ' shows a decreasing trend with A_a, and seems to reach a plateau for $A_a > 0.005$ s^{-1}. Parameter α' also shows an increasing trend with A_a, except for Set A (no ageing).

The comparison between measured and predicted outlet temperatures is shown by means of the overlay plot, shown in Figure 6(a) for the intermediate Set B as example, and the residuals, calculated with Eq. (12) and represented in Figure 6(b) for the all parameter sets (A-F).

$$\varepsilon[\%] = \frac{T_{out}^{sim} - T_{out}}{T_{out}} 100 \tag{12}$$

Consistently with the results of the lack-of-fit test, the residuals in Figure 6(b) are greater for lower values of A_a, especially during the initial 100 days. Then, the pattern in the residuals changes abruptly (short period indicated with dashed-dotted vertical lines), and thereon the system is (approximately) equally well represented by all parameter sets, with the residuals within ±1.5%.

Figure 7(a) shows the calculated *average* fouling resistance for Sets A-F (continuous lines) calculated with Eq. (7) with Mode I. The *apparent* fouling resistance (calculated directly from plant data with Mode III-A, see Figure 4a) is also plotted in Figure 7(a), for comparison (dashed line). The overall thermal resistance is similar for different combinations of γ'-A_a. For no ageing (Set A), the apparent falling rate is result of a combination of decreasing film temperature and increasing wall shear stress due to deposit build-up. As the ageing rate increases, the conductivity of the deposit increases faster over time. This is also reflected as an apparent falling rate as measured by the fouling resistance. As a result, a smaller deposition-offsetting effect is required to explain the same thermal fouling resistance for greater values of A_a.

The trend observed in the residuals is again evidenced by comparing apparent and average resistances, with the greatest mismatch noted in the initial 100 days and reasonably good match thereon. The most significant difference in behaviour is observed in the short period indicated with vertical dashed-dotted lines, during which the apparent resistance decreases and the average resistances increase.

Further insights are obtained from plotting the tube-side flowrate (Figure 7b). The change in trend observed in the residuals coincides with a low-flow period (between vertical lines). This explains the increase in fouling rate predicted by the model as the deposition-offsetting term decreases with shear stress (negative term in Eq. (9)), thus with flowrate. The behaviour observed in the apparent resistance, however, contradicts the well-known functionality of crude oil fouling rate on velocity in the threshold

model: fouling resistance decreases despite the very low velocities. This explains, in part, the mismatch between model and data and the change in trend. The results seem to indicate that other external factors not considered by the correlation are playing a significant role during the initial period (e.g. characteristics of the fluids, non-recorded operations such as bypasses, or simply the deposition model not capturing completely well the behaviour of the system at very low shears).

Based on the above discussion, it can be concluded that the thermal performance can be explained with similar accuracy for different combinations of ageing and deposition-offsetting parameters. Differences in the residuals seem to be related to wrong functionality in the deposition rate or uncertainties in the plant data. On the other hand, the pressure drop predicted for the various cases differs significantly, as shown in Figure 8. ΔP becomes extremely high for fast ageing, and only Sets A-C (A_a = 0 – 0.003 s^{-1}) lead to realistic hydraulic performance. In addition, it should be noted that, as demonstrated in this example, a better fit does not imply necessarily a more correct model.

Average thickness and effective conductivity

The predicted average deposit thickness is significantly different for Sets A-E (Figure 9a), leading to the difference in pressure drop previously noted. For no ageing (Set A) the thickness reaches a maximum value of 1.33 mm, whilst for fast ageing (Set E) the thickness at the end of the period is 3.8 mm, heavily blocking the tube. Deposit thicknesses reported in literature[13] range between 1.0-2.8 for the most fouled unit (av. 1.6 mm). As a result, only the predictions for Sets A-C, with thicknesses at the end of Period 1 ranging between 1.33 – 2.76 mm, seem to lead to realistic values. This is coherent with the previous discussion based on pressure drops.

For comparison, it is possible to plot the *apparent* thickness based on 'measured' duty and fixed conductivity of 0.2 $Wm^{-1}K^{-1}$with Mode II-PP. This value can be compared to the average thickness for the no ageing case (Set A): if the fitting were perfect, the two values would match. The comparison between such apparent thickness for 0.2 $Wm^{-1}K^{-1}$ (dashed line in Figure 9b) and the average thickness for Set A is similar to that previously shown for the fouling resistance. The apparent thickness line shows a finite, non-zero initial thickness of deposit, whilst the model considers clean condition as

starting point. Therefore a heat exchanger not completely clean could also be an additional factor contributing to the mismatch between model and plant data.

This comparison is not possible for Sets B-E, since the thermal-conductivity evolves over time due to ageing. In those cases, the conductivity presents a distribution in the radial direction, along each tube, and is different for each pass and shell. The average effective conductivity that captures the overall contribution of such distribution in a single value (calculated with Eq. 4) is shown in

Figure 10(a). Ageing leads to a gradual increase in the average effective thermal-conductivity, starting from that of fresh organic deposit and gradually leading to that of coke. For the fastest ageing rate, the maximum average effective conductivity observed is 0.65 $Wm^{-1}K^{-1}$, which is still far from that of completely coked deposits (1 $Wm^{-1}K^{-1}$). The radial profiles at the entrance and exit of the exchanger after a year of simulation and for Set E (fast ageing) are shown in

Figure 10(b). The surface of the layer presents lower conductivity, which limits heat transfer through the layer and leads to an average effective conductivity lower than the arithmetic average, as shown in the inset of Figure 10(b).

Consequently, the average effective conductivity of organic deposits, even with very strong ageing, is not expected to exceed 0.5-0.7 $Wm^{-1}K^{-1}$. The final conductivity for Set C is 0.44 $Wm^{-1}K^{-1}$, which is in good agreement with the results in previous sections, where a range of 0.2-0.4 $Wm^{-1}K^{-1}$ was recommended.

Testing parameter portability

The predictive capabilities of the model, with the parameter sets A-E obtained for E05-P1(Table 5), were tested on the other two periods starting from clean conditions: E05-P3 (same unit, future period) and E02-P2 (different unit in a parallel branch, future period). The fouling behaviour and heat exchanger thermo-hydraulic performance is predicted by fixing the fouling/ageing parameters, setting the initial conditions to clean, and using as inputs the time-varying measured inlet conditions (T_{in}, $\dot{m}$). The simulation results are shown in Figure 11.

For E05-P3, the results show very good agreement between the predicted and measured outlet temperatures. The residuals are within ±1.5% for most of period P3. Large errors are observed during

the last 50 days. However, the sharp transition seems to indicate some issue related to operation or change in conditions unknown to the authors. The prediction for Set A gradually diverges from the measurements, a trend that clearly differs from the other parameter sets. The pressure drops for this period, which is longer than P1, goes to very high values. Only the pressure drop predicted with Sets A and B, the two sets with lower A_a (<0.003 s^{-1}), seems to be reasonable at the end of P3.

For E02-P2, the predictions are well within the error interval of ±1.5%. The greatest residuals are observed during the initial stages, which could suggest that the heat exchanger is not starting from complete clean conditions. The pressure drops are within reasonable values for all sets. This is due to the short duration of period P2 compared to P1 and P3, although the difference in the prediction is still substantial towards the end of P2.

Taking into account the results for the three periods (E05-P1/P3 and E02-P2), it can be concluded that the thermal performance is well captured using multiple combinations of ageing and deposition-offsetting parameters not only in estimation, but also in prediction, as long as the operating conditions and fluids are similar. The hydraulic effects predicted by different parameter sets, on the other hand, are quite different. As a result, the combination of thermal and hydraulic responses may be used to decouple the ageing parameter and the deposition-offsetting parameter. Based on the hydraulic analysis previously reported, reasonable pressure drops were observed for A_a < 0.003 s^{-1} (Sets A and B). The deposit average effective conductivity for those cases is lower than 0.4 $Wm^{-1}K^{-1}$.

Evaluation of threshold loci for high shear designs

Current methods for estimation of fouling parameters involve the fitting of threshold models to [11,16]: (i) data for initial fouling rates from laboratory experiments at different velocities/temperatures, in order to identify the threshold loci; or (ii) historical plant data over time, in order to predict future fouling behaviour in support of operations, i.e. used as a deposition or growth law (as in this paper).

The threshold concept draws an imaginary line in the operating conditions of temperature and velocity (or shear) beyond which fouling no longer occurs. The final aim is to design (or operate) heat exchangers in such way that fouling is prevented or significantly reduced. For instance, heat exchangers may be (re)designed with increased number of tube passes or tubes of reduced diameter, providing what

is known as ‘high shear design’ so as to remain in the no-fouling zone. The trade-offs involved in high-shear designs are discussed elsewhere[32]. Accurate determination of the loci is crucial, since a wrong decision in high shear design may be unfruitful, leading to economic losses and operational issues.

Although the threshold concept was originally proposed for initial fouling rates (method i), the fouling rate models fitted to plant data (method ii) are still used by some authors to extract the threshold loci (e.g. ref.[20]). In most works, the threshold models are fitted without taking into account ageing.

Here, by equating the net deposition rate (Eq. 9) to zero, and solving the equation for fixed mass flowrate, it is possible to establish the location of the fouling threshold for the fouling parameter sets in Table 5. The threshold loci are shown in Figure 12 in terms of the film temperature vs. linear velocity plot. The location of the threshold is heavily influenced by the values of the pairs A_a- γ'. The traditional methodology, ignoring ageing, would lead to the conclusion that the threshold loci are that given by the line for Set A (no ageing). The current operation of exchanger E05 for average clean conditions is represented by point (1) in the figure. A mitigation strategy based on operation on the no-fouling side of the threshold loci, leading for instance to a ‘high shear’ condition at point (2) in Figure 12, would prove ineffective if ageing is important (e.g. $A_a >> 0\ s^{-1}$), since point (2) is actually located on the fouling side.

These results reveal the risks of ignoring the ageing process (and in general, the composition of the deposit) when fitting deposition models and in exchanger design/retrofit.

Evaluation of cleaning effectiveness using refinery data

Once the phenomena underlying fouling are well characterized, it is possible to investigate the effectiveness of partial cleaning actions. If the conductivity of the deposit is uniform and time invariant (that is, ageing or other variations in deposit composition are negligible), a decrease of deposit thickness as a result of a cleaning can be directly inferred from the decrease in fouling resistance. However, if the deposit presents a composition (hence conductivity) profile it is necessary to link the reduction in fouling thickness with the composition of the layer so as to match the observed decrease in thermal resistance.

A simple but pragmatic way to model condition-based cleaning for organic deposits undergoing ageing as function of coke fraction is to represent the cleaning rate as proportional to the driving force[24]:

$$n_{Cl,PCk} = k_{Cl,PCk}\left(x_{PCk,coke} - x_{l,coke}\big|_{\tilde{r}_l=1}\right) \quad (13)$$

where k_{PCk} is a rate constant, $x_{PCk,coke}$ represents the efficacy of method k in removing the deposits and $x_{l,coke\ (\tilde{r}_l=1)}$ is the local concentration of coke at the surface of the deposit. Eq. (13) is applied here to simulate the partial cleanings in the schedule in Table 4. The cleaning characteristic parameters are, of course, unknown and need to be estimated. The rate constant is simply fixed to a value sufficiently high so as to achieve the desired cleaning effectiveness within the corresponding cleaning period. As a result, $x_{PCk,coke}$ remains as the only unknown parameter. The introduction of this rate model permits the seamless simulation of fouling-chemical cleaning sequences. Here, for the first time, this concept is applied to real refinery data with time-varying inputs and compared to plant measurements.

Effectiveness of chemical cleaning

In order to obtain $x_{PCk,coke}$, first the fouling and ageing parameters obtained in the previous sections are fixed so as to simulate the operation period. Second, parameter estimation is used to estimate $x_{PCk,coke}$, the concentration of coke at the deposit surface at the end of the cleaning. This is done by fitting the outlet temperatures of the heat exchanger for the initial two weeks after the end of the cleaning action. This period is long enough to include a number of measurements adequate to capture the change in performance after cleaning (independently of measurement variability), but short enough to avoid significant influence of the re-started fouling deposition process.

The method is applied to establish the effectiveness of the following partial cleanings (Table 4): E02-PC1 after period P2; and E05-PC1 after period P1. To illustrate, the analysis is performed only for the fouling parameter Set B. The results of the parameter estimation are shown in Table 6. Both t-test and lack-of-fit were passed. The residuals with respect to the outlet temperatures are very low, within ±0.37% on average. The overall improvement in calculated average thickness, fouling resistance,

hydraulic performance is also reported in the table. The change in apparent fouling resistance (calculated with Mode III-A, Figure 4) is also reported, for completeness.

For unit E05 the best estimate of the concentration of coke at the surface after the partial cleaning is of 11.2%. This corresponds to a removal of 24% of the deposit thickness, a reduction in the thermal resistance of 40%, and a decrease in $\Delta P/\Delta P_c$ of 0.8. This result compares reasonably well with the decrease in apparent fouling resistance (45.8%). If no ageing is considered, the estimated decrease in deposit thickness is also 45.8%. Therefore, the effectiveness of the cleaning, in terms of thickness, varies between 24-45.8%, depending on whether ageing is considered or not.

For unit E02 the best estimate of the concentration of coke at the surface after the partial cleaning E02-PC1 is only 6%. The thickness removed by the cleaning action is almost identical to that in E05. $\Delta P/\Delta P_c$ decreases by 0.73 while the corresponding reduction in fouling resistance is 37.8%, slightly lower in percentage compared to E05, but greater in absolute terms (2.89 vs. 2.80 $m^2K\ kW^{-1}$). The reduction in average fouling resistance is very similar to than in the apparent one (37.8% vs. 36.1%). Consequently, the decrease in deposit thickness varies from 36.1% without ageing to 21% with ageing.

These results seem to indicate that the two cleaning actions led to very similar deposit thickness removal and were probably performed with the same cleaning method. The results show that the above method allows estimating with good accuracy the initial conditions of the deposit layer at the beginning of a new operation period.

Seamless simulation of actual fouling-cleaning sequences

The previous results enable a simulation to be carried out continuously during and beyond the partial cleaning actions. Comparison of model predictions to measurements for the subsequent period will give an idea of how correct is the description of the layer and the partial cleaning, and the estimated conditions after cleaning. For exchanger E02AB the simulation is here limited to the sequence E02-P2, E02-PC1, and E02P3. For exchanger E05AB, the sequence simulated is E05-P1, E05-PC1, E05-P2, E05-TC2 and E05-P3. Partial cleanings are simulated using Eq. (13). Total cleanings are simulated with the cleaning rate below [24]:

$$n_{Cl,TC} = k_{Cl,TC}\delta_l \quad (14)$$

Outlet temperatures, residuals, fouling resistance (average vs. apparent), and pressure drop are shown in Figure 13 and Figure 14 for E05AB and E02AB, respectively. It is shown that it is possible to seamless simulate, in a single run and with the same deposit model, fouling build-up and a mix of intermediate total and partial cleanings as function of the composition of the deposit.

For E05AB, the simulation involves 1121 days of operation (Figure 13), from which only 353 correspond to the estimation period (of fouling and partial cleaning, P1+PC1). The following 768 days are simulated in fully predictive mode. The outlet temperatures show good agreement with the plant data (Figure 13a). The residuals are within ±1.5% for most of the period (Figure 13b). The greatest deviations are observed at the beginning of P1 (as commented earlier) and at the end of P2 and P3. The last two have in common being sub-periods the highest shear, as evidenced in the pressure drop (Figure 13d). However, the residuals are contradictory, and therefore it is not possible to reach a conclusion on the underlying cause. This is also reflected in the comparison between the apparent resistance (obtained with Mode III-A) and the average resistance from the simulation (Figure 13c).

For E02AB, the simulation involves 768 days (Figure 14). Only the initial data points of period P2 where used in estimation. The rest is fully predicted with the fouling parameters from E05. The predicted outlet temperatures show good agreement with the measurements (Figure 14a) and the residuals are within the admissible 1.5% error for the entire simulated interval (Figure 14b). The comparison between apparent and average resistance show good initial agreement after the partial cleaning (Figure 14c). After 700 days (60 days after PC1), the simulated resistance starts deviating from the apparent one and thereon shows a different trend. The average resistance increases quickly, then stabilizes, and finally starts decreasing due to accumulated ageing. The latter fact is evidenced by the $\Delta P/\Delta P_c$ ratio (Figure 14d), which stabilizes but does not decrease (no removal) in the final stages of period P2. In contrast, the apparent resistance shows (overall) a monotonic increasing trend. Nevertheless, this difference is within the measurement error and good agreement can be considered. It is concluded that it is possible to predict the behaviour of E02 for a very long operating time, beyond partial cleaning, and within an estimation error of less than 1.5% in outlet temperatures.

Finally, the $\Delta P/\Delta P_c$ ratio stays within reasonable values for the two units and the entire simulation periods (Figure 13d, Figure 14d). This hydraulic prediction gives excellent confidence on the quality of the estimated fouling parameters and in their use within this modelling framework to study the impact of fouling and cleaning on both thermal and hydraulic performance, to predict fouling behaviour after a cleaning and to assist in cleaning scheduling.

Conclusions

A complete modelling framework has been presented that brings together various models developed in previous works, some new formulations, and a method for the analysis and characterization of fouling and cleaning of heat exchangers based on thermal and hydraulic performance.

Based on typical industrial field data, and in the absence of pressure drop measurement, the methodology has been shown to provide a systematic approach to: a) evaluating the fouling state of the units based on thermal measurements; b) identifying the range of deposit conductivity that leads to realistic pressure drops; c) estimating key fouling and ageing parameters; d) estimating the effectiveness of cleaning and surface conditions after a clean; e) predicting thermal performance with good accuracy in the outlet temperatures for other periods/exchangers operating in similar conditions.

The study has shown that is possible to explain the same thermal behaviour, both in estimation and prediction, with different combinations of ageing and fouling parameters. This emphasizes the need of moving beyond a simplistic description of the deposit as a fouling resistance. Neglecting the composition of the deposit, in this case due to the gradual ageing of the organic material, may lead to significant deviations in the prediction of pressure drops and wrong identification of the threshold loci. This may have severe consequences if the fouling parameters are used to propose mitigation options such as high shear designs.

For the ageing rates considered, the hydraulic impact of fouling is extremely different, and therefore pressure drop measurements should be considered as a way of “anchoring” (or, at least, narrowing down) the thermal behaviour. If pressure drops and temperatures are both available, they can be potentially used in combination to extract the characteristic thickness and conductivity of the fouling

system over time. This gives powerful insights into potential fouling causes, deposition rates as a function of operating conditions, and variations in deposit composition due to phenomena such as ageing. In addition, when the proposed deposition and ageing models provide a good description of the system, these measurements may be used in parameter estimation to decouple ageing from fouling parameters.

With a proposed dependency of partial cleaning on deposit state such as given by Eq. 13 or similar, the use of the models and method to simulate partial removal and fouling resumption under time-varying inputs has been demonstrated. Parameter estimation has been applied to assess the cleaning effectiveness, in terms of deposit removed and state of the deposit left after partial cleaning (e.g. concentration of coke remaining at the layer surface). The main practical result is the ability to estimate the degree of cleaning, and deposit state, at the beginning of a new operation period, and to seamlessly simulate sequences of fouling and (full or partial) cleaning. This was demonstrated by simulating the performance of unit E02 for 768 days and one intermediate partial cleaning and that of unit E05 for 1121 days and two intermediate cleanings (one partial and one complete). The error in the calculated outlet temperatures is within ±1.5% for most of the periods. Deviations observed for some particular periods point to other factors such as changes in feedstock or non-recorded use of bypasses to be the underlying cause. In addition, these deviations are observed either at very low or very high shear, which might indicate that the dependency on shear stress in the fouling correlation used is not completely correct.

In practical terms, the excellent accuracy demonstrated in full prediction mode gives a great confidence in using the approach presented to assist in planning of cleaning schedules and mitigation actions.

Acknowledgments

This research was partially performed under the UNIHEAT project. EDB and SM wish to acknowledge the Skolkovo Foundation and BP for financial support. The support of Hexxcell Ltd, through provision of Hexxcell Studio™, is also acknowledged.

Notation

A	=	Analysis solution type
A_a	=	Ageing pre-exponential factor, s^{-1}
ANN	=	Artificial neural network
API	=	API gravity
b_{clean}	=	Sum of cleaning binary variables for all cleaning methods
b_k	=	Cleaning binary variable for method *k*
c	=	Mass concentration, kg m^{-3}
C_p	=	specific heat capacity, J kg^{-1} K^{-1}
D_i	=	Inner tube diameter, m
D_o	=	Outer tube diameter, m
D_s	=	Shell diameter, m
E_a	=	Ageing activation energy, J mol^{-1}
E_f	=	Fouling deposition activation energy, J mol^{-1}
h	=	Tube-side heat transfer coefficient, W m^{-2} K^{-1}
$k_{Cl,PC,k}$	=	Cleaning rate constant of partial cleaning method *k*, kg m^{-2} s^{-1}
$k_{Cl,TC}$	=	Cleaning rate constant of total cleaning method, kg m^{-3} s^{-1}
L	=	Tube length, m
$LMTD$	=	Log mean temperature difference method
$\dot{m}$	=	Mass flowrate, kg s^{-1}
$MeABP$	=	Mean average boiling point, ^{0}C
$n_{Cl,k}$	=	Cleaning rate of method k, kg m^{-2} s^{-1}
$n_{f,i}$	=	Fouling rate of component i, kg m^{-2} s^{-1}
NC	=	Number of components
NCl	=	Number of cleaning methods
N_p	=	Number of passes
NR	=	Number of reactions

N_s = Number of shells

N_t = Number of tubes

P = Prediction solution type

PC = Partial cleaning

PP = Pressure drop prediction solution type

Pr = Prandtl number

Q = Heat duty, W

$q"$ = Heat flux, W m^{-2}

QP = Heat duty prediction solution type

R_{flow} = Flow radius, m

R_i = Inner tube radius, m

R_o = Outer tube radius, m

Re = Reynolds number

R_f = Fouling resistance, m^2 K W^{-1}

R_g = Ideal gas constant, J mol^{-1} K^{-1}

r = Radial coordinate, m

$\tilde{r}$ = Dimensionless radial coordinate

r_j = Rate of reaction j, kg m^{-3} s^{-1}

T = Temperature, K

TC = Total cleaning

T_{film} = Tube-side film temperature, K

t = Time, s

u = Tube-side velocity, m s^{-1}

U = Overall heat transfer coefficient, W m^{-2} K^{-1}

x = Volume fraction, m^3 m^{-3}

$x_{PCk,coke}$ = Maximum fraction of coked deposit removable by method PCk

z = Axial coordinate, m

Greek letters

α' = Deposition constant, kg m^{-2} s^{-1}

γ' = Deposition-offsetting constant, kg m^{-2} s^{-1} Pa^{-1}

ΔP = Tube-side pressure drop, Pa

δ_l = Fouling layer thickness, m

$\dot{\delta}_l$ = Rate of change of fouling layer thickness, m s^{-1}

ε = Residual, %

$\varepsilon - \mathrm{NTU}$ = Effectiveness – Number of transfer units method

ρ = Density, kg m^{-3}

λ = thermal conductivity, W m^{-1} K^{-1}

ν_{ij} = Stoichiometric coefficient for component i in reaction j

$\nu_{38°C}$ = kinematic viscosity at 38^0C, mm^2 s^{-1}

τ_w = Wall shear stress, N m^{-2}

Ω = Spatial domain

Subscripts

a = Ageing; apparent deposit characteristics (thickness and conductivity)

ave = Average

c = Clean conditions

coke = Aged organic deposit

Cl = Cleaning

eff = Effective

gel = Fresh organic deposit

i = Component number

in = Inlet

j = Reaction number

l = Fouling layer

n = Pass number

PCk = Partial chemical cleaning type k

TC = Total cleaning

out = Outlet

s = Shell

t = Tube-side flow

w = Tube wall

Literature Cited

1. Coletti F, Joshi HM, Macchietto S, Hewitt GF. Introduction to Crude Oil Fouling. In: Coletti F, Hewitt GF, eds. *Crude Oil Fouling: Deposit Characterization, Measurements, and Modeling*. Boston: Gulf Professional Publishing; 2014.

2. Macchietto S, Hewitt GF, Coletti F, et al. Fouling in Crude Oil Preheat Trains: A Systematic Solution to an Old Problem. *Heat Transf Eng*. 2011;32(3-4):197-215.

3. Müller-Steinhagen H, Malayeri MR, Watkinson a. P. Heat Exchanger Fouling: Mitigation and Cleaning Strategies. *Heat Transf Eng*. 2011;32(3-4):189-196.

4. Müller-Steinhagen H, Zettler HU. *Heat Exchanger Fouling: Mitigation and Cleaning Technologies*. 2nd Ed. Essen, Germany: PP Publico; 2011.

5. Coletti F, Macchietto S. Refinery Pre-Heat Train Network Simulation Undergoing Fouling: Assessment of Energy Efficiency and Carbon Emissions. *Heat Transf Eng*. 2011;32(3-4):228-236.

6. Markowski M, Trafczynski M, Urbaniec K. Identification of the influence of fouling on the heat recovery in a network of shell and tube heat exchangers. *Appl Energy*. 2013;102:755-764.

doi:10.1016/j.apenergy.2012.08.038.

7. Coletti F, Crittenden BD, Haslam AJ, et al. Modelling of Fouling from Molecular to Plant Scale. In: Coletti F, Hewitt GF, eds. *Crude Oil Fouling: Deposit Characterization, Measurements, and Modeling*. Boston: Gulf Professional Publishing; 2014.

8. Ebert WA, Panchal CB. Analysis of Exxon crude-oil-slip stream coking data. In: Panchal CB, ed. *Fouling Mitigation of Industrial Heat-Exchange Equipment*. San Luis Obispo, California (USA): Begell House; 1995:451-460.

9. Deshannavar UB, Rafeen MS, Ramasamy M, Subbarao D. Crude oil fouling a review. *J Appl Sci*. 2010;10(24):3167-3174.

10. Wang Y, Yuan Z, Liang Y, Xie Y, Chen X, Li X. A review of experimental measurement and prediction models of crude oil fouling rate in crude refinery preheat trains. *Asia-Pacific J Chem Eng*. 2015;10:607-625.

11. Wilson DI, Ishiyama EM, Polley GT. Twenty years of Ebert and Panchal - What next? In: *Proc. Int. Conf. Heat Exchanger Fouling and Cleaning - 2015*. Vol 2015. Enfield (Dublin), Ireland; 2015:1-12.

12. Takemoto T, Fellow BDC, Fellow STK. Interpretation of fouling data in industrial shell and tube heat exchangers. *Trans IChemE*. 1999;77(8):769-778.

13. Crittenden BD, Kolaczkowski ST, Downey IL. Fouling of Crude Oil Preheat Exchangers. *Trans IChemE, Part A, Chem Eng Res Des*. 1992;70:547-557.

14. Heins A, Veiga R, Ruiz C, Riera A. Fouling Monitoring and Cleaning Optimisation in a Heat Exchanger Network of a Crude Distallation Unit. *Proc 7th Int Conf Heat Exch Fouling Clean - Challenges Oppor*. 2007;RP5(1925).

15. Mirsadraee A, Malayeri MR. ANALYSIS OF HIGHLY NOISY CRUDE OIL FOULING

DATA USING KALMAN FILTER. In: Malayeri MR, Müller-Steinhagen H, Watkinson AP, eds. *Proc. Int. Conf. Heat Exchanger Fouling and Cleaning - 2015*. Enfield (Dublin), Ireland; 2015:97-103.

16. Yeap BL, Wilson DI, Polley GT, Pugh SJ. Mitigation of crude oil refinery heat exchanger fouling through retrofits based on thermo-hydraulic fouling models. *Chem Eng Res Des*. 2004;82(1):53-71.

17. Polley GT, Wilson DI, Pugh SJ, Petitjean E. Extraction of Crude Oil Fouling Model Parameters from Plant Exchanger Monitoring. *Heat Transf Eng*. 2007;28(3):185-192.

18. Ishiyama EM, Heins AV, Paterson WR, Spinelli L, Wilson DI. Scheduling cleaning in a crude oil preheat train subject to fouling: Incorporating desalter control. *Appl Therm Eng*. 2010;30(13):1852-1862.

19. Ratel M, Kapoor Y, Anxionnaz-Minvielle Z, Seminel L, Vinet B. Investigation of fouling rates in a heat exchanger using an innovative fouling rig. In: Malayeri MR, Müller-Steinhagen H, Watkinson AP, eds. *Proc. Int. Conf. Heat Exchanger Fouling and Cleaning - 2013*. Budapest, Hungary; 2013:36-41.

20. Costa ALH, Tavares VBG, Borges JL, et al. Parameter Estimation of Fouling. *Heat Transf Eng*. 2013;34(8-9):683-691.

21. Radhakrishnan VR, Ramasamy M, Zabiri H, et al. Heat exchanger fouling model and preventive maintenance scheduling tool. *Appl Therm Eng*. 2007;27(17-18):2791-2802.

22. Aminian J, Shahhosseini S. Neuro-based formulation to predict fouling threshold in crude preheaters. *Int Commun Heat Mass Transf*. 2009;36(5):525-531.

23. Kashani MN, Aminian J, Shahhosseini S, Farrokhi M. Dynamic crude oil fouling prediction in industrial preheaters using optimized ANN based moving window technique. *Chem Eng Res Des*. 2012;90(7):938-949. doi:10.1016/j.cherd.2011.10.013.

24. Diaz-Bejarano E, Coletti F, Macchietto S. A new dynamic model of crude oil fouling deposits and its application to the simulation of fouling-cleaning cycles. *AIChE J*. 2016;62(1):90-107.

25. Chenoweth JM. General Design of Heat Exchangers for Fouling Conditions. In: Melo LF, Bott TR, Bernardo CA, eds. *Fouling Science and Technology*. Vol 145. NATO ASI Series. Springer Netherlands; 1988:477-494. doi:10.1007/978-94-009-2813-8_32.

26. Coletti F, Macchietto S. A Dynamic, Distributed Model of Shell-and-Tube Heat Exchangers Undergoing Crude Oil Fouling. *Ind Eng Chem Res*. 2011;50(8):4515-4533.

27. Process Systems Enterprise. gPROMS. 2016. http://www.psenterprise.com/gproms.html.

28. Ishiyama EM, Paterson WR, Wilson DI. Thermo-hydraulic channelling in parallel heat exchangers subject to fouling. *Chem Eng Sci*. 2008;63(13):3400-3410.

29. Polley GT, Morales-Fuentes A, Wilson DI. Simultaneous Consideration of Flow and Thermal Effects of Fouling in Crude Oil Preheat Trains Simultaneous Consideration of Flow and Thermal Effects of Fouling. *Heat Transf Eng*. 2009;30(10-11):815-821. doi:10.1080/01457630902751494.

30. Ishiyama EM, Paterson WR, Wilson DI. The Effect of Fouling on Heat Transfer, Pressure Drop, and Throughput in Refinery Preheat Trains: Optimization of Cleaning Schedules. *Heat Transf Eng*. 2009;30(10-11):805-814.

31. Coletti F, Macchietto S, Polley GT. Effects of fouling on performance of retrofitted heat exchanger networks: A thermo-hydraulic based analysis. *Comput Chem Eng*. 2011;35(5):907-917.

32. Coletti F, Diaz-Bejarano E, Martinez J, Macchietto S. Heat exchanger design with high shear stress: reducing fouling or throughput? In: *International Conference on Heat Exchanger Fouling and Cleaning - 2015*. Enfield (Ireland); 2015.

33. Diaby LA, Lee L, Yousef A. A Review of Optimal Scheduling Cleaning of Refinery Crude Preheat Trains Subject to Fouling and Ageing. *Appl Mech Mater*. 2012;148-149:643-651.

34. Ishiyama EM, Paterson WR, Wilson DI. Optimum cleaning cycles for heat transfer equipment undergoing fouling and ageing. *Chem Eng Sci*. 2011;66(4):604-612.

35. Ishiyama EM, Coletti F, Macchietto S, Paterson WR, Wilson DI. Impact of Deposit Ageing on Thermal Fouling : Lumped Parameter Model. *AIChE J*. 2010;56(2):531-545.

36. Gillham CR, Fryer PJ, Hasting APM, Wilson DI. Cleaning-in-Place of Whey Protein Fouling Deposits. *Food Bioprod Process*. 1999;77(June):127-136. doi:10.1205/096030899532420.

37. Hexxcell Ltd. Hexxcell Studio. http://www.hexxcell.com. Published 2016.

38. Sinnot RK. *Coulson and Richardson's Chemical Engineering; Volume 6, Chemical Engineering Design*. 3rd ed. Oxford: Butterworth Heinemann; 1999.

39. Henry J. Headers, Nozzles, and Turnarounds. In: Hewitt GF, ed. *Heat Exchanger Design Handbook*. Redding (USA): Begell House; 2008.

40. Albert F, Augustin W, Scholl S. Roughness and constriction effects on heat transfer in crystallization fouling. *Chem Eng Sci*. 2011;66(3):499-509.

41. Wilson DI, Watkinson AP. A study of autoxidation reaction fouling in heat exchangers. *Can J Chem Eng*. 1996;74:236-246.

42. Turakhia M, Characklis WG, Zelver N. Fouling of Heat Exchanger Surface: Measurement and Diagnosis. *Heat Transf Eng*. 1984;5(July 2015):93-101. doi:10.1080/01457638408962772.

43. Riazi MR. *Characterization and Properties of Petroleum Fractions*. 1st ed. Philadelphia: ASTM; 2005.

44. Diaz-Bejarano E. A Reaction Engineering Approach to Modelling of Crude Oil Fouling

Deposits: Analysis, Monitoring and Cleaning. 2016.

45. Panchal CB, Kuru WC, Liao CF, Ebert WA, Palen JW. Threshold conditions for crude oil fouling. In: Bott TR, Melo LF, Panchal CB, Somerscales EFC, eds. *Understanding Heat Exchanger Fouling and Its Mitigation*. NY: Begell House; 1999:273-279.

46. Watkinson AP. *Critical Review of Organic Fluid Fouilng.*; 1988.

47. Coletti F, Ishiyama EM, Paterson WR, Wilson DI, Macchietto S. Impact of Deposit Aging and Surface Roughness on Thermal Fouling : Distributed Model. *AIChE J*. 2010;56(12):3257-3273.

48. Diaz-Bejarano E, Coletti F, Macchietto S. Crude oil Fouling Deposition, Suppression, Removal and Consolidation - and how to tell the difference. *Heat Transf Eng*. 2016:Accepted for Publication.

49. Franceschini G. New Formulations for Model-Based Experiment Design and Application to a Biodiesel Production Process. 2007.

List of Figures

Table 1: Equations and boundary conditions for the four deposit modes

Deposit Layer (Ω_l)	**Mode I**	**Mode II**	**Mode III**	**Mode IV**
Energy Balance	$\rho_{l,n}(z,r)C_{p,l,n}(z,r)\frac{\partial T_{l,n}(z,r)}{\partial t} = \frac{1}{r}\frac{\partial}{\partial r}\left(r\lambda_{l,n}(z,r)\frac{\partial T_{l,n}(z,r)}{\partial r}\right)$		-	-
Energy Balance boundary condition(s)	$\dot{q}_{w,n}\big\|_{r=R_i}(z) = \dot{q}_{l,n}\big\|_{r=R_i}(z)$ $T_{w,n}\big\|_{r=R_i}(z) = T_{l,n}\big\|_{r=R_i}(z)$ $\dot{q}_{l,n}\big\|_{r=R_{flow,n}}(z) = h_n(z)\left(T_n(z) - T_{l,n}\big\|_{r=R_{flow,n}}(z)\right)$		$\dot{q}_{w,n}\big\|_{r=R_i}(z) = \frac{\left(T_n(z) - T_{w,n}\big\|_{r=R_i}(z)\right)}{\left(\frac{1}{h_n(z)} + R_f\right)}$	$\dot{q}_{w,n}\big\|_{r=R_i}(z) = h_n(z)\left(T_n(z) - T_{w,n}\big\|_{r=R_i}(z)\right)$
Flow Radius	$R_{flow,n}(z) = R_i - \delta_{l,n}(z)$	$R_{flow} = R_i - \delta_a$	$R_{flow} = R_i$	$R_{flow} = R_i$
Dimensionless coordinate	$\tilde{r}_{l,n} = \frac{R_i - r}{\delta_{l,n}(z)}$	$\tilde{r}_l = \frac{R_i - r}{\delta_a}$	-	-
Local Conductivity	$\lambda_{l,n}(z,r) = \sum_{i=1}^{NC} x_{l,i,n}(z,r)\lambda_i$	$\lambda_a = const$	-	-
Mass Balance	$\left(\frac{\partial c_{l,i}(z,\tilde{r}_l)}{\partial t} - \frac{\tilde{r}_l}{\delta_l(z)}\dot{\delta}_l(z)\frac{\partial c_{l,i}(z,\tilde{r}_l)}{\partial \tilde{r}_l}\right) = \sum_{j=1}^{NR} v_{ij}r_j(z,\tilde{r}_l)$ Boundary condition: See ref.[24]	-	-	-

Table 2: Inputs and outputs to the heat exchanger for the various deposit modes and solution types

Solution types		**Mode I**	**Mode II**	**Mode III**	**Mode IV**
Prediction (P)	Inputs	$(T_{in}, \dot{m})_{s,t}$,	$(T_{in}, \dot{m})_{s,t}$, δ_a, λ_a	$(T_{in}, \dot{m})_{s,t}$, R_f	$(T_{in}, \dot{m})_{s,t}$
	Fouling rate	$\dot{\delta}_l$, $c_{l,i(r = Rflow)}$*	-	-	-
	Outputs	Q, ΔP	Q, ΔP	Q, ΔP_c	Q_c, ΔP_c
Analysis (A)	Inputs	-	$(T_{in}, \dot{m})_{s,t}$, Q, ΔP	$(T_{in}, \dot{m})_{s,t}$, Q	-
	Outputs	-	δ_a, λ_a	R_f, ΔP_c	-
***Q*-Prediction**	Inputs	-	$(T_{in}, \dot{m})_{s,t}$, ΔP , λ_a	-	-
(QP)	Outputs	-	Q , δ_a	-	-
Δ*P*-Prediction	Inputs	-	$(T_{in}, \dot{m})_{s,t}$, Q , λ_a	-	-
(PP)	Outputs	-	ΔP , δ_a	-	-

Note: subscripts *in, s, t, c* and *a* refer to inlet, shell, tube, clean and apparent. *Concentration of foulant species *i* at the deposit surface, given by the deposit mass balance boundary condition.

Table 3: Main geometric[5], average overall heat transfer coefficient and tube-side velocity in clean conditions, and fluids physical properties parameters for E02AB. Same parameters apply to E05AB.

Parameter	**Value**	**Parameter**	**Tube fluid**	**Shell Fluid**
N_s	2	Fluid	Crude Oil	Residuum
Arrangement	Parallel flow	API	35	18.4
N_p	4	MeABP (ºC)	233	588
D_s (mm)	1397	$\nu_{38ºC}$ ($mm^2\ s^{-1}$)	5.5	200
D_i (mm)	19.86			
D_o (mm)	25.4			
N_t	880			
$u_{c,\ ave}$ ($m\ s^{-1}$)	2			
$U_{c,\ ave}$ ($W\ m^{-2}\ K^{-1}$)	436			

Table 4: Operation and cleaning schedule for E02AB and E05AB (entries in parenthesis after each period are their duration in days).

E02AB	**P1 (332 d)**		**TC1**	**P2 (286 d)**	**PC1**	**P3 (456 d)**	**PC2**
E05AB	TC1	P1 (349 d)	PC1	P2 (268 d)	TC2	P3 (495 d)	

P: Operating period; PC: Partial Cleaning; TC: Total cleaning

Table 5: Parameter estimation results for E05AB-P1.

Set	Fixed	Optimal Estimate		χ^2	95% t-value		Corr.
	A_a (s^{-1})	α' (kg $m^{-2}s^{-1}$)	$10^9\gamma'$ (kg $m^{-2}s^{-1}Pa^{-1}$)		α'	γ'	
A	0	1.32 ± 0.11	15.5 ± 2.2	579	205.4	7.23	0.99**
B	0.0015	1.00 ± 0.08	3.6 ± 1.2	335	228.2	3.02	0.97**
C	0.003	1.07 ± 0.07	1.8 ± 0.9	257	266.5	1.9	0.96
D	0.005	1.20 ± 0.07	1.2 ± 0.8	209	311.7	1.57*	0.94
E	0.010	1.49 ± 0.07	1.3 ± 0.6	167	389.7	2.13	0.91
Reference value for statistics				738		1.65	

Note: density of the deposit assumed that of asphalt (2360 kg m^{-3}); *$t < t_{ref}$, low confidence in the value; **high correlation.

Table 6: Parameter estimation results of cleaning effectiveness for PC1 of E02 and E05 and Set B.

Heat Exchanger – Cleaning	**E02 – PC1**	**E05 – PC1**
Parameter estimation results		
Optimal Estimate $x_{PCk,coke}$	0.060 ± 0.023	0.112 ± 0.021
95% t-value (ref 1.67)	2.589	5.373
χ^2 (ref 64.0)	16.8	11.2
ε (%) (ave.)	±0.14	±0.37
Improvement in calculated average variables ([1]: before cleaning; [2]: after cleaning)		
$\delta_{ave,[1]} - \delta_{ave,[2]}$ (mm)	-0.54	-0.54
$(\delta_{ave,[1]} - \delta_{ave,[2]})/\delta_{ave,[1]}$ (%)	-26.1	-24.0
$\Delta R_{f.ave[1]} - \Delta R_{f.ave[2]}$ ($m^2K\ kW^{-1}$)	-2.89	-2.8
$(\Delta R_{f.ave[1]} - \Delta R_{f.ave[2]})/\Delta R_{f.ave[1]}$ (%)	-37.8	-40.0
$(\Delta P_{[1]} - \Delta P_{[2]} \cdot \Delta P_{c[1]} / \Delta P_{c[2]})/\Delta P_{[1]}$ (%)	80	73
Improvement in apparent R_f (Figure 4a) ([1]: before cleaning; [2]: after cleaning)		
$(\Delta R_{f[1]} - \Delta R_{f[2]})/\Delta R_{f[1]}$ (%)	-36.1	-45.8

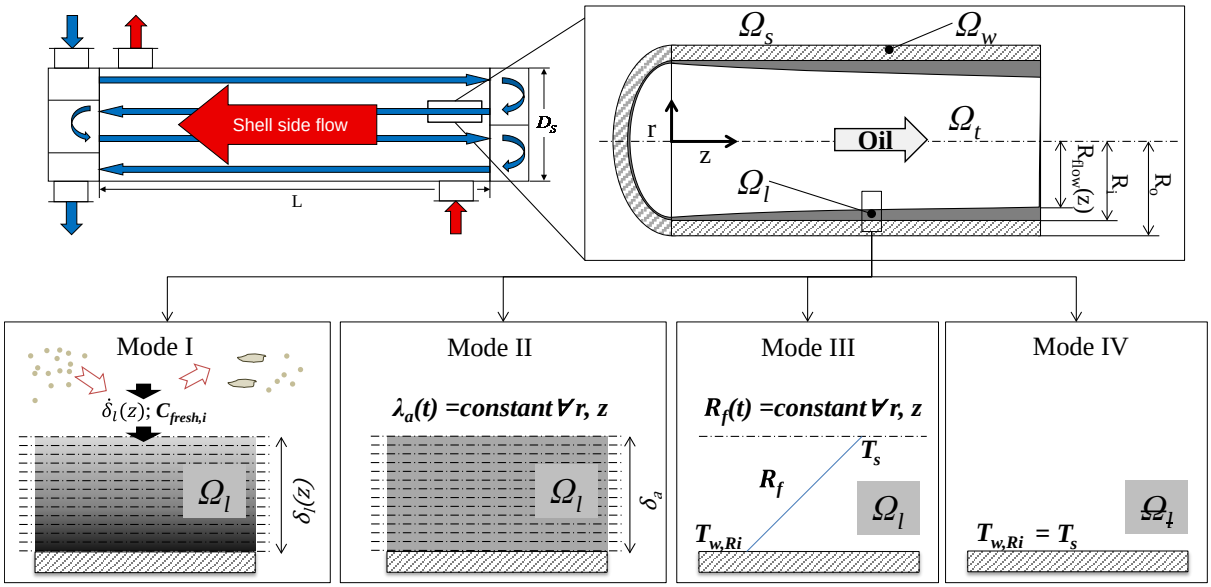

Figure 1: Schematic representation of heat exchanger model[26] and deposit Modes I - IV.

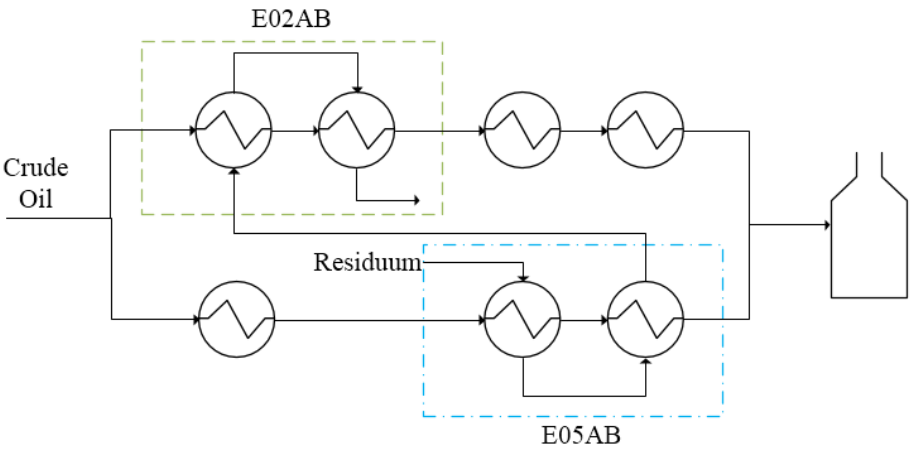

Figure 2: Location of E02 and E05 in the network (adapted from ref.[5]).

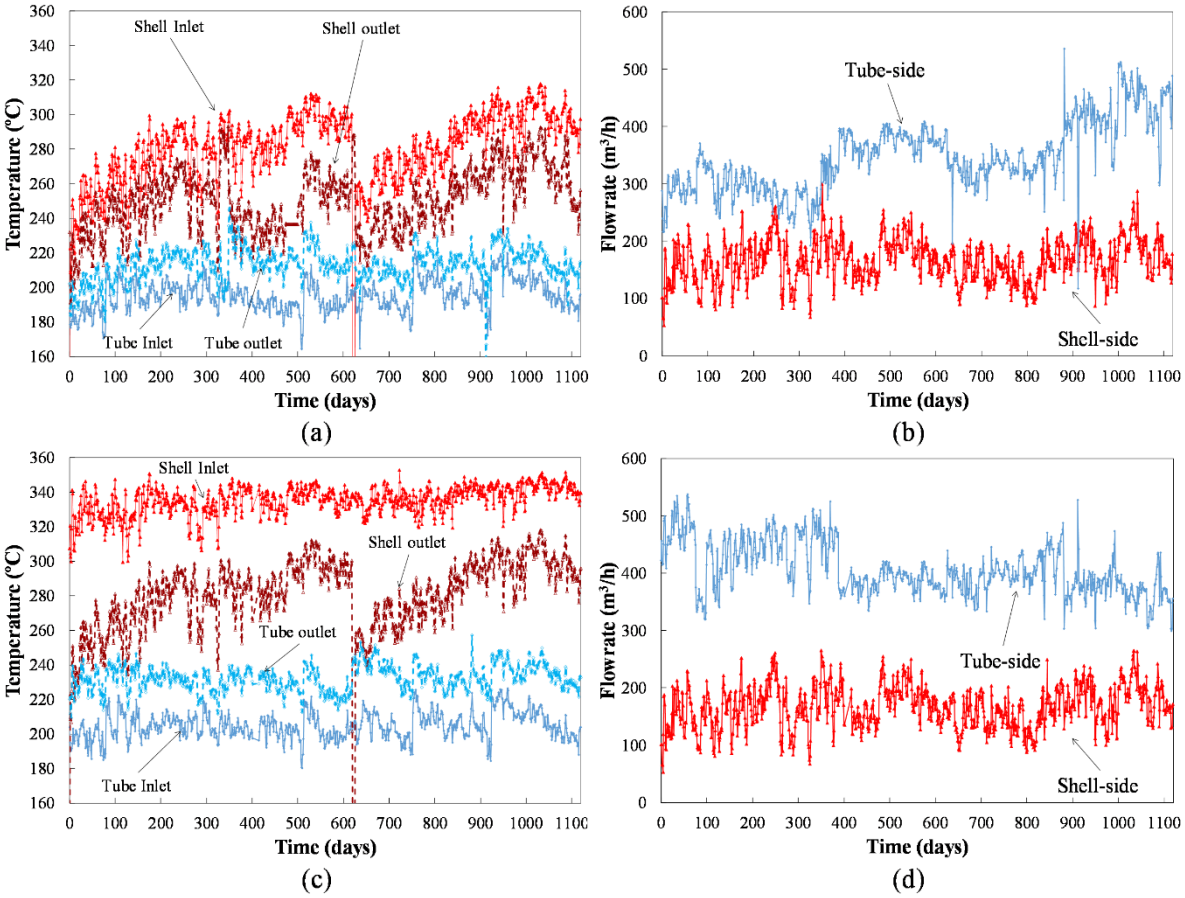

Figure 3: Inlet and outlet temperatures and flowrates for E02AB (a, b) and E05AB (c, d).

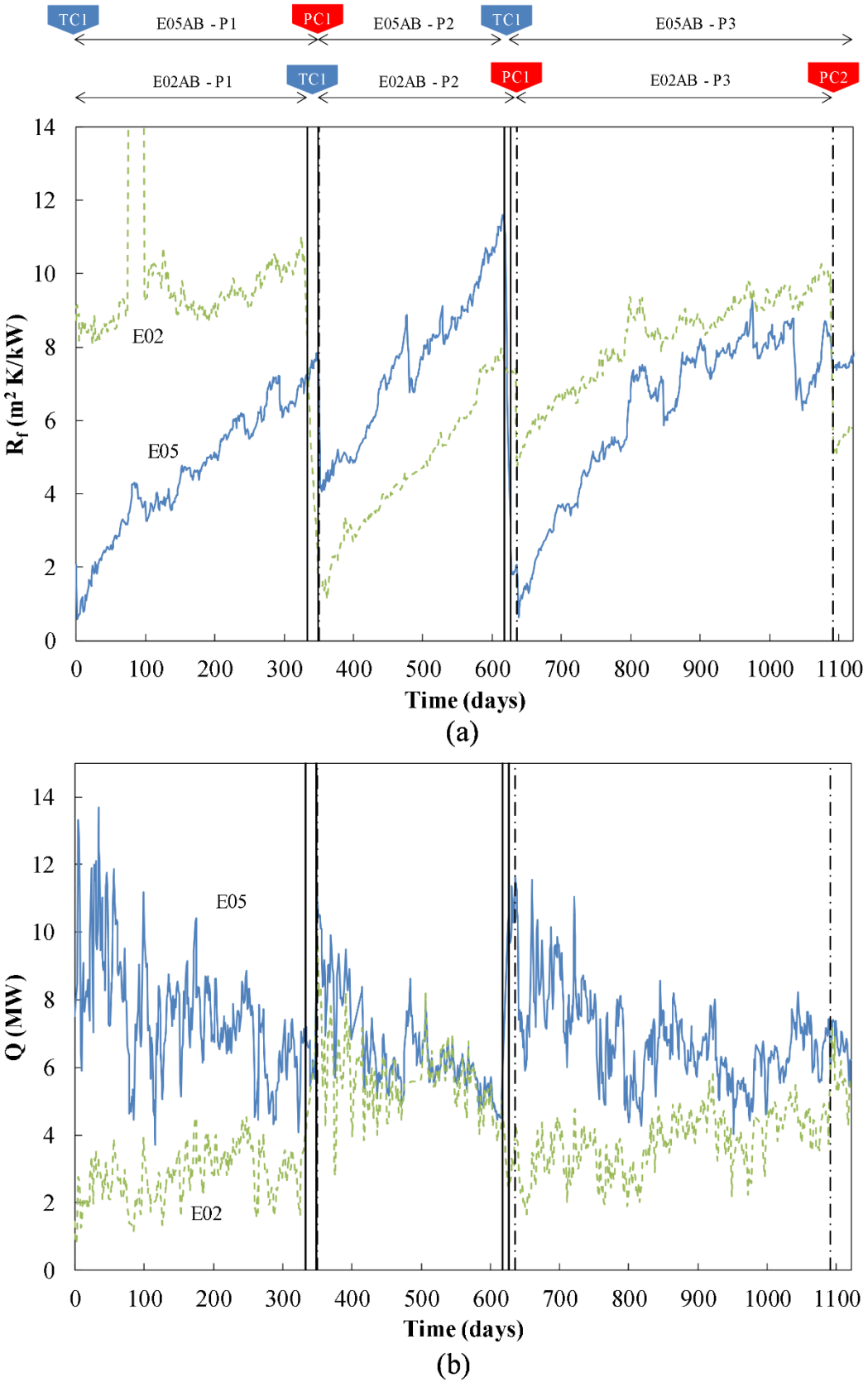

Figure 4: Apparent fouling resistance (a) and heat duty (b) over time for E02AB (dashed) and E05AB (continuous).

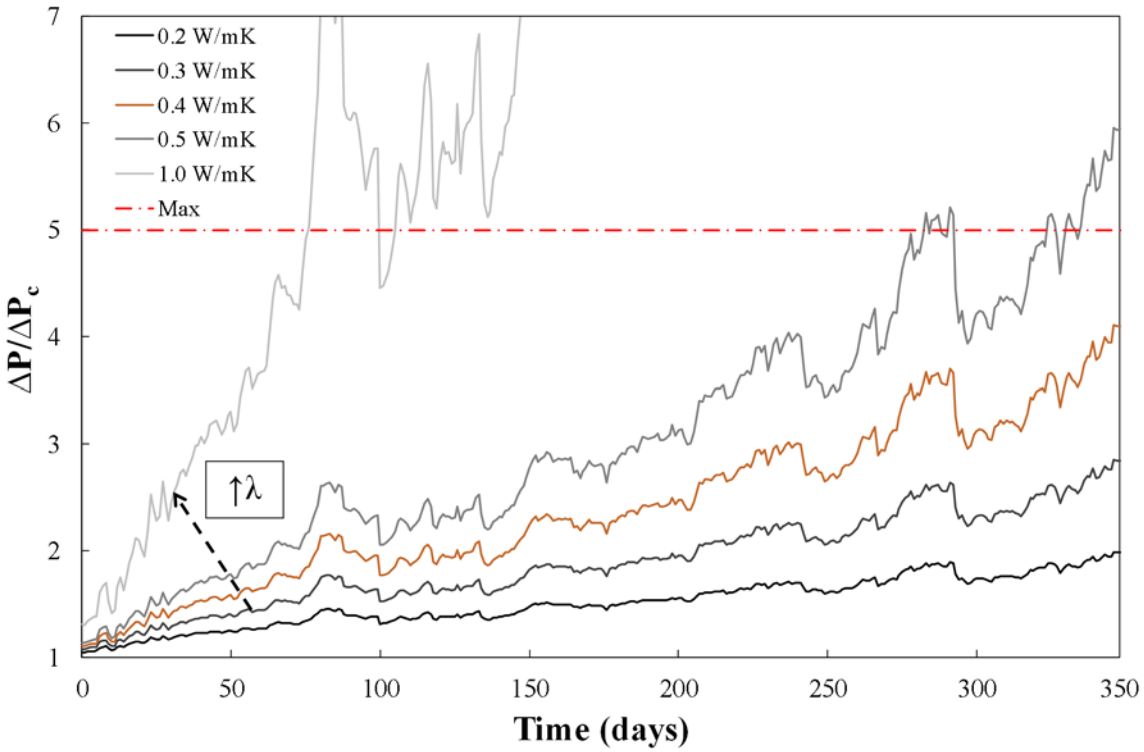

Figure 5: Predicted ratio $\Delta P/\Delta P_c$ by using Mode II-PP and various apparent conductivities.

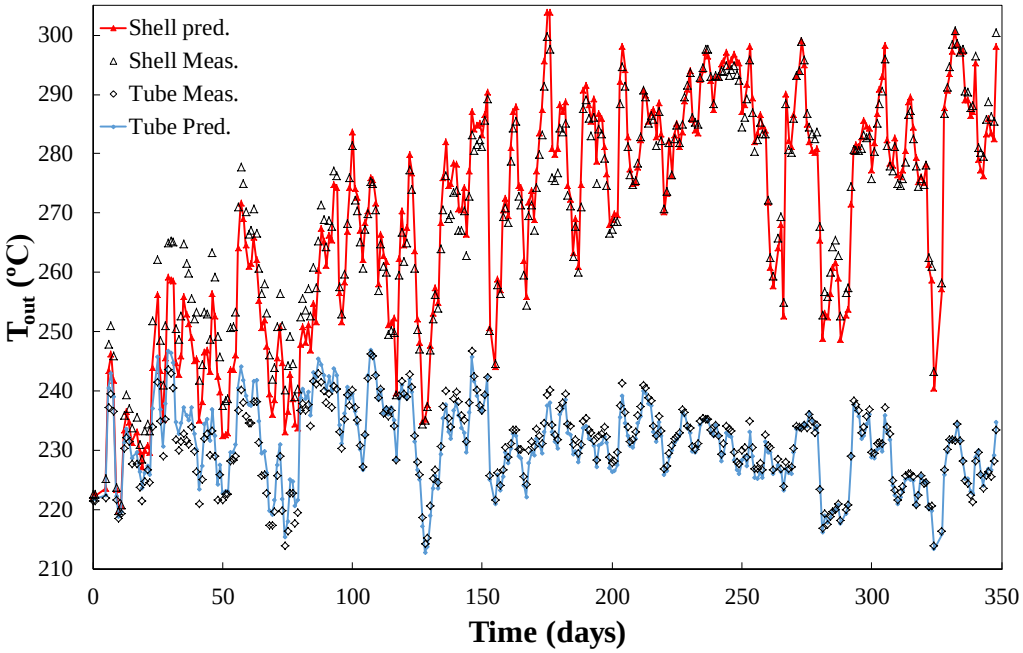

(a)

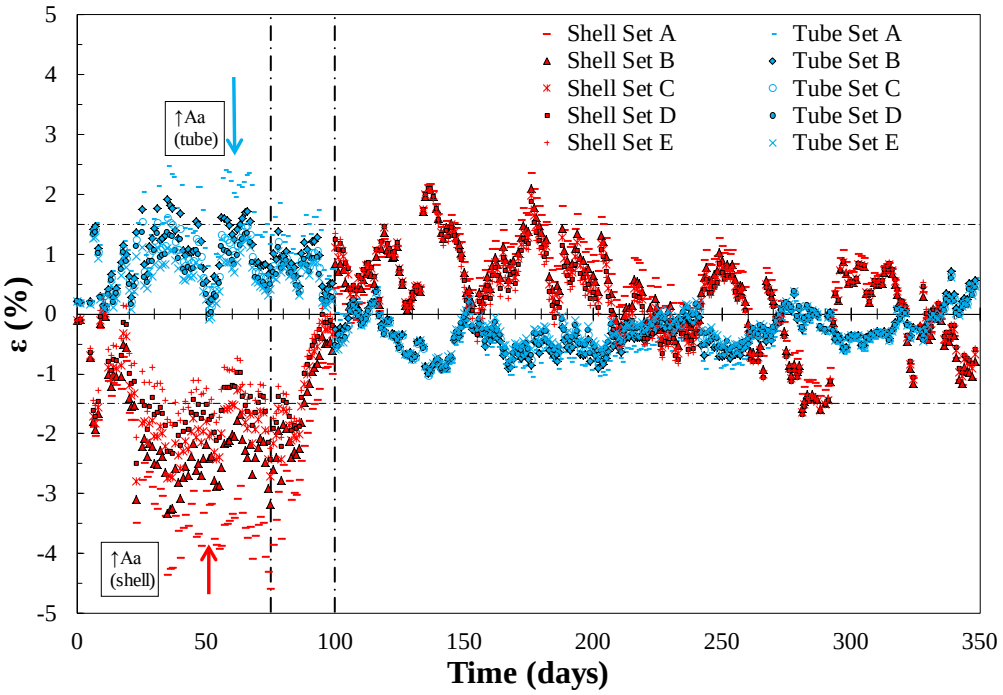

(b)

Figure 6: Overlay Plot for E05-P1 for Set B (a) and Residuals for Sets A-E (b). Vertical dashed-dotted lines indicate a low-flow period.

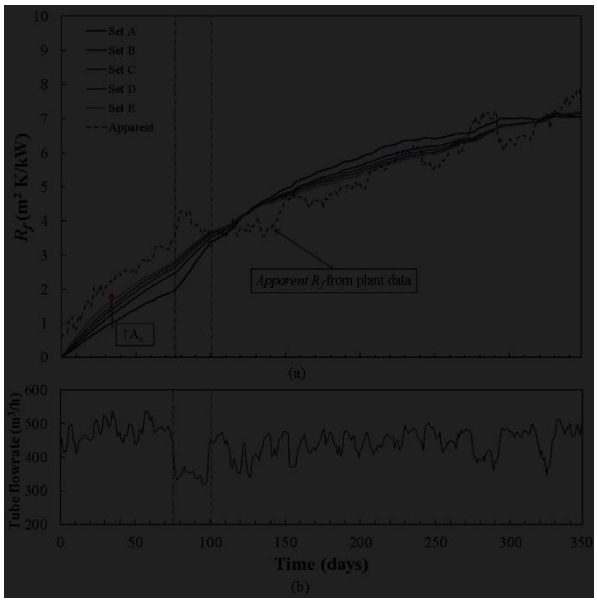

Figure 7: Estimation Period E05-P1: (a) Average R_f for Sets A-E and apparent R_f (Mode III-A); (b) tube-side flowrate. Vertical dashed-dotted lines indicate a low-flow period.

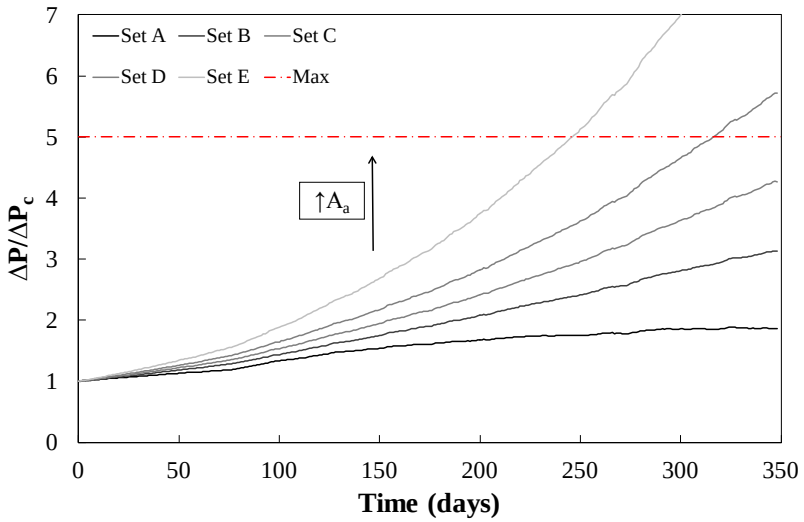

Figure 8: Estimation period E05-P1: $\Delta P/\Delta P_c$, for Sets A-E.

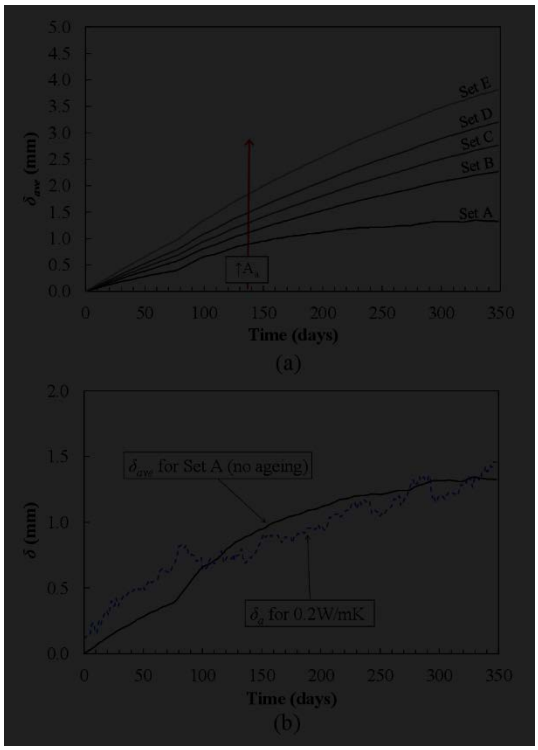

Figure 9: Average thickness for Sets A-E (E05P1) (a) and comparison between average thickness for Set A and apparent thickness for 0.2 $Wm^{-1}K^{-1}$ (Mode II-PP).

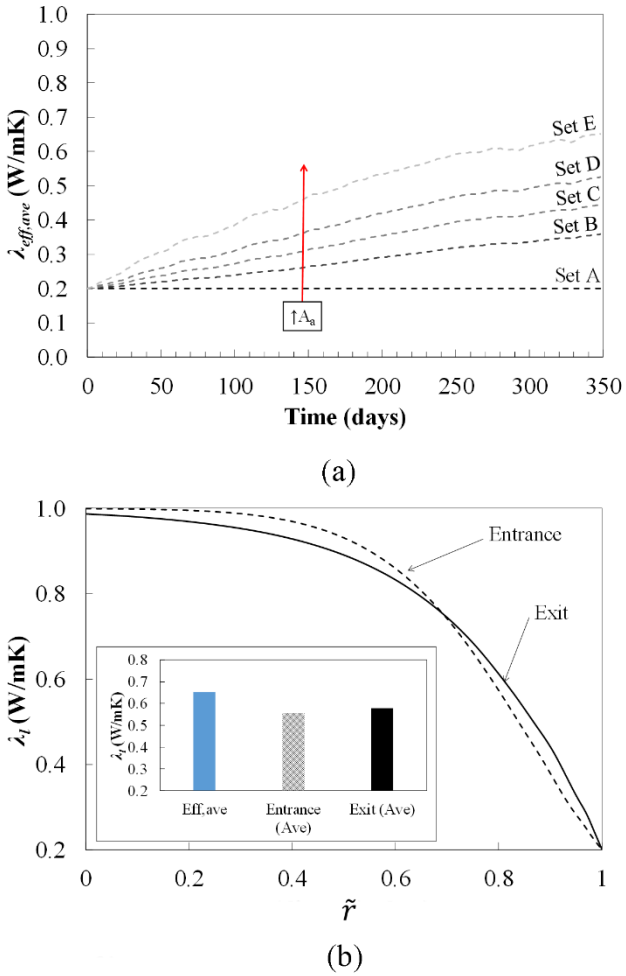

Figure 10: E05-P1: Average effective conductivity for Sets A-E (a); local conductivity radial profile at entrance and exit of E05AB after a year of simulation, for Set E. In the inset, comparison of effective and arithmetic average conductivity and entrance and exit (b).

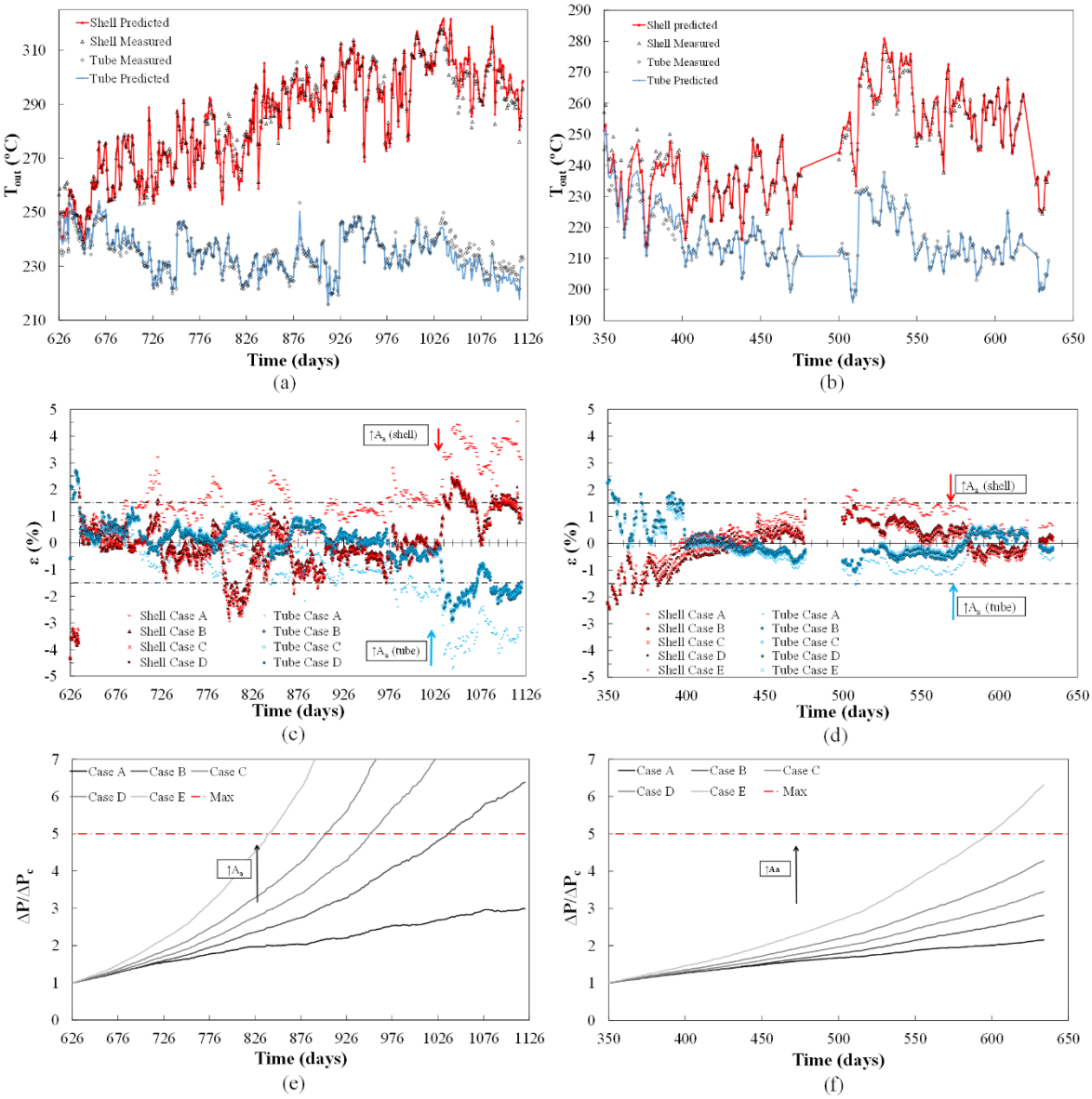

Figure 11: Testing for portability of estimated parameters: outlet temperatures for Set B, residuals and predicted pressure drops for Sets A-E in E05–P3 (a, c, e) and E02-P2 (b, d, f).

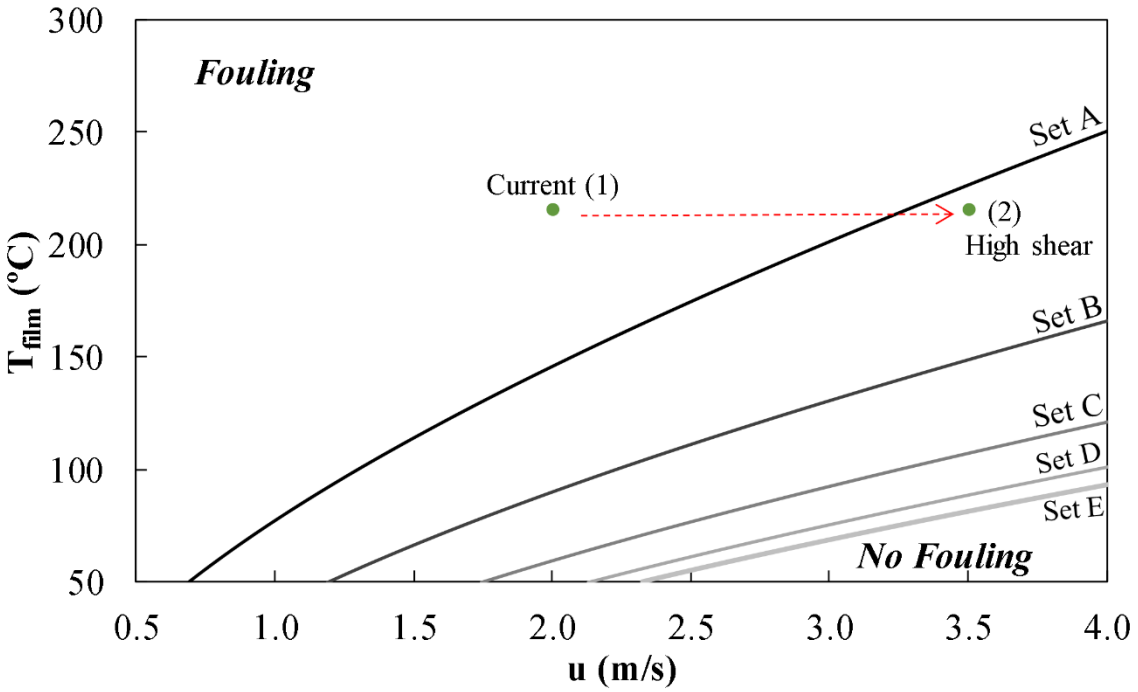

Figure 12: Threshold loci for E05 and parameter sets A-E. Point (1) represents current average operating conditions (clean) and point (2) a high shear to mitigate fouling.

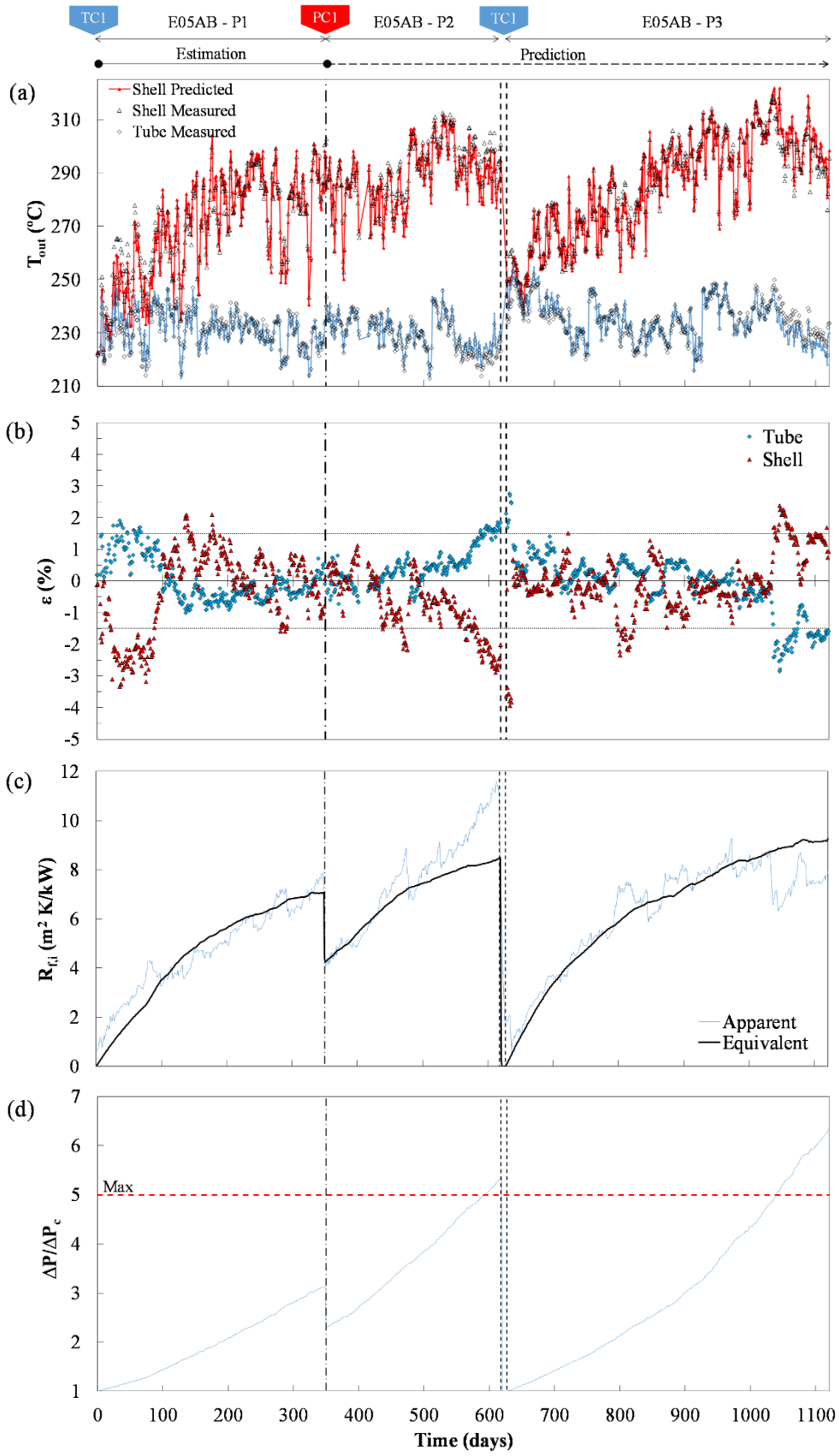
TC1
E05AB - P1
PC1
E05AB - P2
TC1
E05AB - P3
Estimation
Prediction
(a)
Shell Predicted
Shell Measured
Tube Measured
T_{out} (ºC)
(b)
Tube
Shell
ε (%)
(c)
R_{fi} (m² K/kW)
Apparent
Equivalent
(d)
Max
ΔP/ΔP$_c$
Time (days)

Figure 13: Seamless simulation of E05 operation schedule (P1-P3): outlet temperatures (a), residuals (b), thermal resistance (c) and pressure drop normalized to clean values (d).

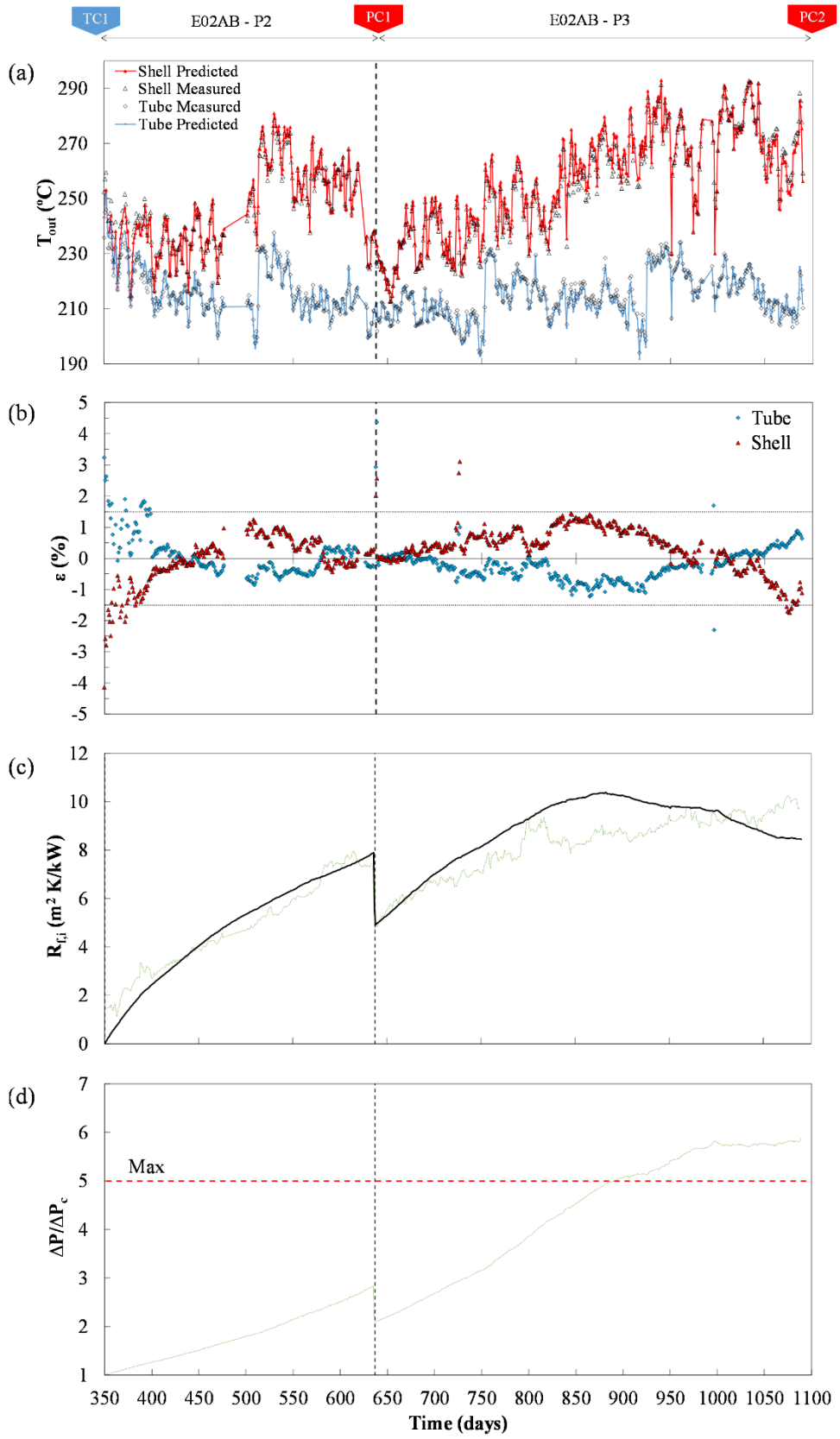

Figure 14: Seamless simulation of E02 operation schedule (P2-P3): outlet temperatures (a), residuals (b), thermal resistance (c) and pressure drop normalized to clean values (d).